电 化 学
J. Electrochem. 2022, 28(11), 2219004 (1 of 23)

[Review] DOI: 10.13208/j.electrochem.2219004 http://electrochem.xmu.edu.cn

Review on Oxygen-Free Vanadium-Based Cathodes for Aqueous Zinc-Ion Batteries

Xiao-Ru Yun, Yu-Fang Chen*, Pei-Tao Xiao*, Chun-Man Zheng*

(*College of Aerospace Science and Engineering, National University of Defense Technology, Changsha, Hunan, 410073, China*)

Abstract: Aqueous zinc-ion batteries (AZIBs) are considered as one of the most promising next-generation electrochemical energy storage systems owing to their high-power density, environmental benign, intrinsic safety, and the low cost of the abundant zinc resources. However, their further development is still plagued by the inferior electrochemical performance of cathode materials. Though extensive research has been conducted to investigate various cathode materials (including manganese oxides, vanadium oxides, Prussian blues analogy, and organic materials), design of high-performance cathodes with satisfying capacity and long-term cycling stability still faces great challenges. Oxygen-free vanadium-based compounds, owing to their better conductivity, larger interlayer spacing, lower ion diffusion barrier and higher theoretical specific capacity than those of vanadium oxides, have gained increasing attention recently. In this review, we summarize the recent development about the emerging oxygen-free vanadium-based compounds in AZIBs, emphasizing the methods to design electrode materials with desired structures, effective strategies to improve their electrochemical performance, and the fundamental electrochemical mechanisms. Finally, the current challenges and outlooks of oxygen-free vanadium-based compounds are proposed, providing a novel perspective and useful guidance for the design of high-performance vanadium-based cathode materials for AZIBs.

Key words: zinc-ion batteries; oxygen-free vanadium-based compound; energy storage mechanisms; electrochemical performance

1 Introduction

With the increasing attention to global environmental issues, development of new energy storage/conversion systems with high performance is, though challenging, urgently needed[1, 2]. Among various energy storage/conversion systems, lithium-ion batteries, as a type of commercial battery, are extensively employed in portable electronic products, electric vehicle power pack and large-scale energy storage systems owing to their broad potential window, excellent cycle stability, and relative high energy density[3-8]. Nevertheless, the limited metal resources (high cost) and flammable organic electrolytes (high safety risk) severely impede further application of lithium-ion batteries, which, in turn, has inspired researchers to pay their attention to aqueous metal-ion batteries with low cost, safety and easy preparation (Na^+, K^+, Zn^{2+}, Mg^{2+}, Al^{3+}, etc.)[8, 9].

Among various aqueous metal-ion batteries, aqueous zinc-ion batteries (AZIBs) have been widely investigated due to the following advantages: (1) lower redox potential (-0.762 V vs. S.H.E.), (2) high theoretical gravimetric (820 $mAh \cdot g^{-1}$) and volumetric (5855 $mAh \cdot cm^{-3}$) capacities, and (3) better stability

Cite as: Yun X R, Chen Y F, Xiao P T, Zheng C M. Review on oxygen-free vanadium-based cathodes for aqueous zinc-ion batteries. *J. Electrochem.*, 2022, 28(11): 2219004.

Received: 2022-09-06, Revised: 2022-09-30. * Corresponding author, Tel: (86-731)87007201, E-mail: chenyufang@nudt.edu.cn, xiaopt@nudt.edu.cn, zhengchunman@nudt.edu.cn

in aqueous electrolyte (higher overpotential for hydrogen evolution)[4, 10, 11]. However, traditional alkaline ZIBs have two main issues that affect the electrochemical performance. On the one hand, Zn dendrites are easily generated on the surface of Zn metal anodes, which may penetrate the separator, resulting in rapid capacity failure and even short circuit of the battery[12, 13]. Great progresses have been achieved to suppress Zn dendrites via design of novel Zn composites anode, engineering of current collectors, and regulations of electrolytes and electrode-electrolyte interphases. On the other hand, the cathode materials are often prone to be dissolved in the electrolyte, which also leads to rapid capacity fading during the long-term electrochemical process[4]. To address those issues, extensive studies have been made to develop AZIBs with advanced cathode materials, such as manganese-based oxides, Prussian blue analogs, organic compounds and vanadium-based compounds, etc. [7,14,15]. Although manganese-based materials exhibit high theoretical capacity, poor cycling stability is induced by the irreversible structural degradation during charge-discharge process.

Recently, our group, taking advantages of the porous nature and large specific surface area of carbon-based composite, has prepared the conductive carbon-coated manganese oxides (C-MnO_2) derived from MOFs, which improved the cycle performance of MnO_2[16]. Specifically, compounding the electrode material with the MOF framework boosts the stability of the structure, mitigating the collapse of the structure during cycling. Moreover, the stable carbon framework effectively inhibits the dissolution of MnO_2 in the electrolyte and improves the ion transport efficiency. Additionally, the porous structure can also provide additional active sites for ion/electron diffusion, shortening the ion/electron transport pathway and improving the efficiency of Zn^{2+} ions de/intercalation. Consequently, C-MnO_2//Zn AZIBs exhibited a high specific capacity of 234 mAh·g^{-1} at a current density of 0.2 A·g^{-1} and an excellent long-term cycling stability with a capacity retention of 81% at 1 A·g^{-1} after 1000 cycles. Prussian Blue analogs, benefiting from the open lattice structural framework with tunable pore size, can effectively alleviate the huge volume expansion during the cycling process, but the inherent low theoretical capacity impedes their practical application[8]. Our group firstly synthesized an organ-ometallic framework porous cathode material (Ni-PTA-Mn) with large specific surface area and excellent electrical conductivity by a one-step hydrothermal method. Benefiting from the hydrogen bond network in the skeletal structure and the reversible proton conductivity, the electrode exhibited high specific capacity (139 mAh·g^{-1} at 0.1 A·g^{-1}) and impressive long-term cycling life (93% capacity retention over 100 cycles at 1 A·g^{-1})[17]. In addition, organic compounds have superior reversibility and wide voltage windows. However, the issues about poor cycling life and low conductivity need to be addressed before their further application[18]. By comparison, vanadium-based compounds possess a more promising development potential than the above compounds, because they have typical layered structure and rich valence states, as well as significantly higher energy density and theoretical capacity[3,4,12]. Various types of vanadium oxides have been widely studied and summarized in previous reports. Recently, oxygen-free vanadium-based compounds, as one type of the vanadium-based compounds, have emerged as novel cathodes for AZIBs due to their higher electrical conductivity, larger layer spacing and lower ion diffusion barrier[19]. Up to now, the research on oxygen-free vanadium-based compounds is at a relatively early stage, a comprehensive review summarizing the recent development of oxygen-free vanadium-based compounds as cathodes for AZIBs is lacking.

This review is dedicated to providing a comprehensive summary of the research progress on oxygen-free vanadium-based compounds in AZIBs (mainly including vanadium sulfides, vanadium selenide, vanadium nitrides, and other oxygen-free vanadium-based compounds), emphasizing the current status of research on energy storage mechanisms and various effective methods to improve the electrochemical performance, which is outlined in Figure 1. Finally, some reason-

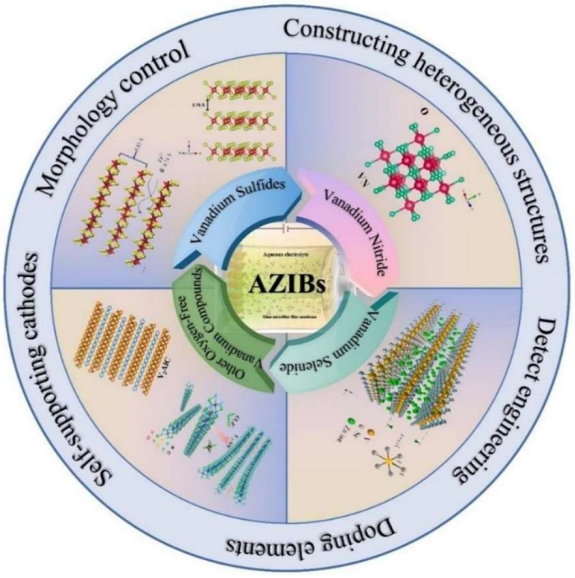

Figure 1 Schematical illustration of the contents emphasized in this review. Reproduced with permission of Ref.[20, 21], copyright 2020 Wiley-VCH. Reproduced with permission of Ref.[22], copyright 2020 Royal Society of Chemistry. Reproduced with permission of Ref. [23], copyright 2021 Elsevier. Reproduced with permission of Ref. [24], copyright 2021 Elsevier. Reproduced with permission of Ref. [25], copyright 2022 American Chemical Society. (color on line)

able insights into the current challenges and future application of oxygen-free vanadium-based compounds are presented, which may shed lights on the development of new oxygen-free vanadium-based AZIBs cathode materials and further practical application of AZIBs.

2 Vanadium Sulfides and their Composites in AZIBs

2.1 VS_2 and Its Composites in AZIBs

VS_2 possesses a typical layered crystal structure and is composed of two S-layers sandwiched by V-layers. The adjacent layers are bound together by weak *van der Waals* forces, rendering an open structure with a large interlayer spacing of 5.76 Å, as shown in Figure 2A[19, 26]. This large interlayer spacing is sufficient to allow the insertion/extraction, and enable rapid ion diffusions of Li^+ (0.69 Å), Zn^{2+} (0.74 Å), Na^+ (1.02 Å), Mg^{2+} (1.32), K^+ (1.33), and even NH^{4+} (1.48 Å). In addition, VS_2 has good metallic properties (conductivity of 5.0×10^2 $S \cdot m^{-1}$) and is expected to be capable of providing faster ion diffusion than molybdenum disulphide and graphite, both of which also possess the layered crystal structures[3]. Based on these advantages, VS_2, with its novel and complex electronic structure, has attracted tremendous attention as a promising cathode material for ZIBs.

He et al.[19] first synthesized the VS_2 nanosheets by a simple hydrothermal approach, and then fabricated the AZIBs with a zinc foil anode (Figure 2B). As exhibited in Figure 2C, nanosheets with a thickness of 50 ~ 100 nm were assembled into VS_2 bouquet. The VS_2 nanosheets showed a reversible capacity of 190.3 $mAh \cdot g^{-1}$ at 0.05 $A \cdot g^{-1}$ in the voltage range of 0.4 ~ 1 V and excellent long-term cycling stability with a capacity retention of 98% at 0.5 $A \cdot g^{-1}$ after 200 cycles. As shown in Figure 2D, the *ex-situ* X-ray diffraction (XRD) results display that the intensity and position of the characteristic peak of VS_2 at 15.4° gradually decreased with the progress of discharge, indicating that the interlayer spacing of the (001) plane was expanded as a result of the insertion of Zn^{2+} ions. Conversely, the peak magnitude and peak location gradually went back to the initial state when charged to 1 V, corresponding to the zinc ion extraction process. The evolution of XRD during the discharge-charge process indicated that the Zn^{2+} ions de/intercalation during charging/discharging is fully reversible. Moreover, the results obtained by *ex-situ* transmission electron microscopy/high-resolution transmission electron microscopy (TEM/HRTEM), *ex-situ* selected area electron diffraction (SAED) spectroscopy, *in-situ* Raman spectroscopy and *ex-situ* X-ray photoelectron spectroscopy (XPS) were in good agreement with the *in-situ* XRD results. In summary, the electrochemical reactions of Zn//VS_2 AZIBs can be proposed as follows:

Cathode:

$$VS_2 + 0.09Zn^{2+} + 0.18e^- \leftrightarrow Zn_{0.09}VS_2 \quad (1)$$

$$Zn_{0.09}VS_2 + 0.14Zn^{2+} + 0.28e^- \leftrightarrow Zn_{0.23}VS_2 \quad (2)$$

Anode:

$$Zn^{2+} + 2e^- \leftrightarrow Zn \quad (3)$$

In order to rationally control the inherent Zn^{2+}

insertion/extraction behavior within VS_2, it is important to understand relationship between energy storage mechanism and potential range. Tan et al.[27] prepared unique 1T-VS_2 nanospheres by assemble of thin nanosheets. The abundant active sites and stable structure in the 1T-VS_2 nanospheres promoted rapid electron/ion diffusion and improved the cycling stability of the VS_2 nanospheres. Furthermore, as exhibited in Figure 2E-K, it was found that compared with that at 1.0 V, there were residual incompletely removed Zn^{2+} ions between the VS_2 layers when charged to 0.85 V. It is speculated that these Zn^{2+} ions might act as "pillars" to strengthen the stability of layered structure in VS_2, thus ensuring the highly

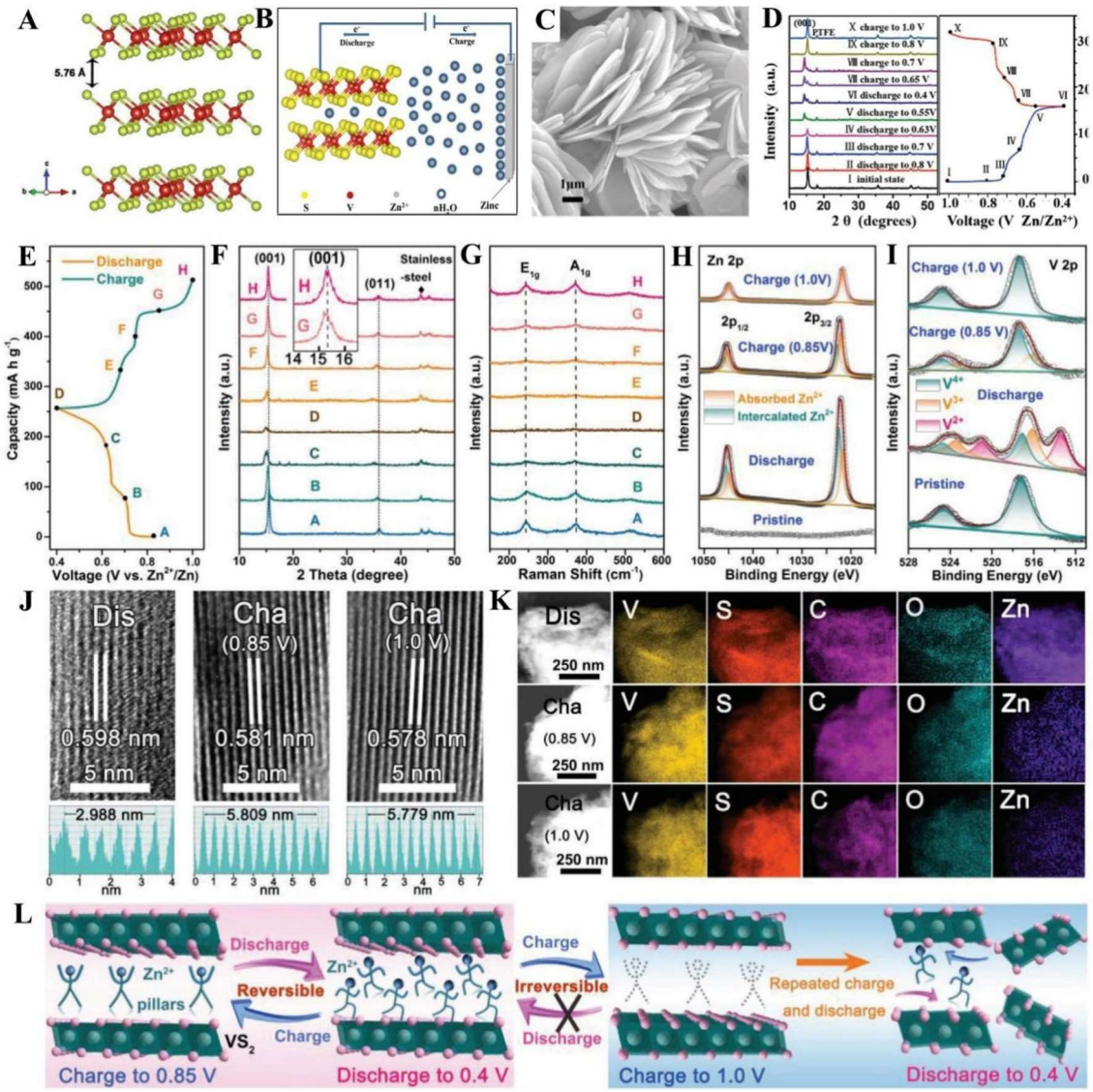

Figure 2 (A) Schematic crystal structure of the VS_2. Reproduced with permission of Ref.[20], copyright 2020 Wiley-VCH. (B) Schematic illustration for the operation mechanism of Zn//VS_2 ZIBs. (C) The SEM image of layered VS_2. (D) *Ex-situ* XRD patterns of VS_2 collected at various states. Reproduced with permission of Ref.[19], copyright 2017 Wiley-VCH. (E) Charge-discharge curve of VS_2 nanospheres within 0.4 ~ 1.0 V at 0.1 A·g^{-1} in the first cycle. *Ex-situ* (F) XRD patterns with magnified signals at the G and H states (inset), (G) Raman spectra, and XPS spectra of (H) Zn 2p and (I) V 2p. (J) HRTEM images and the corresponding contrast line profiles, and (K) STEM element mapping images of VS_2 nanospheres at various charge/discharge states. (L) Schematic illustration of the Zn-ion storage mechanisms on layered VS_2 under the charge cut-off voltages of 0.85 V and 1.0 V. Reproduced with permission of Ref.[27], copyright 2022 Wiley-VCH. (color on line)

reversible Zn^{2+} insertion/extraction behavior and the structure stability during the cycling process, as schematically illustrated in Figure 2L. As a result, the VS_2 nanospheres delivered a capacity of 212.9 mAh·g^{-1} at 0.1 A·g^{-1} with the excellent cycling performance of 93.3% and 86.7% at 0.5 and 2 A·g^{-1} after 100 and 2000 cycles, respectively (in the voltage range of 0.4 ~ 0.85 V). In contrast, the VS_2 nanospheres cathode faced severe structural degradation when cycling at a voltage range of 0.4 ~ 1 V, demonstrating the key role of the Zn^{2+} located in the VS_2 interlayer as "pillars" played in strengthening the VS_2 laminate structural stability. This discovery redefines the concept of "dead Zn^{2+}", which is generally considered to be detrimental to electrochemical performance, and broadens the prospects for layered oxygen-free vanadium-based cathode for AZIBs.

It is widely accepted that some disadvantages of vanadium-based materials, such as their tendency to be dissolved in the electrolyte and the large volume changes during cycling, have a severe impact on electrochemical performance[14, 28, 29]. In recent years, studies have demonstrated that vanadium-based composites and carbon materials can effectively address the above problems. This approach has also been extensively investigated in vanadium-based oxides in AZIBs, such as V_2O_5/graphene[30], $V_2O_5 \cdot nH_2O$/graphene[31], RGO/VO_2[32], $H_2V_3O_8$/rGO nanowires[33], and $Na_3V_2(PO_4)_3$/rGO[34]. In particular, our group has also carried out some work on modifying vanadium oxide materials with carbon materials. Li et al.[35] used the strategy of *in-situ* growth of MOF derived V_2O_3 on carbon cloth to prepare V_2O_3-CC cathode. Combined with the oxygen vacancy and the stability of MOF structure, the as-fabricated V_2O_3-CC//Zn AZIBs showed high specific capacity (447 mAh·g^{-1} at 0.1 A·g^{-1}) and excellent cycle stability (~100% capacity retention over 5000 cycles at 1 A·g^{-1}, with a reversible capacity of 203

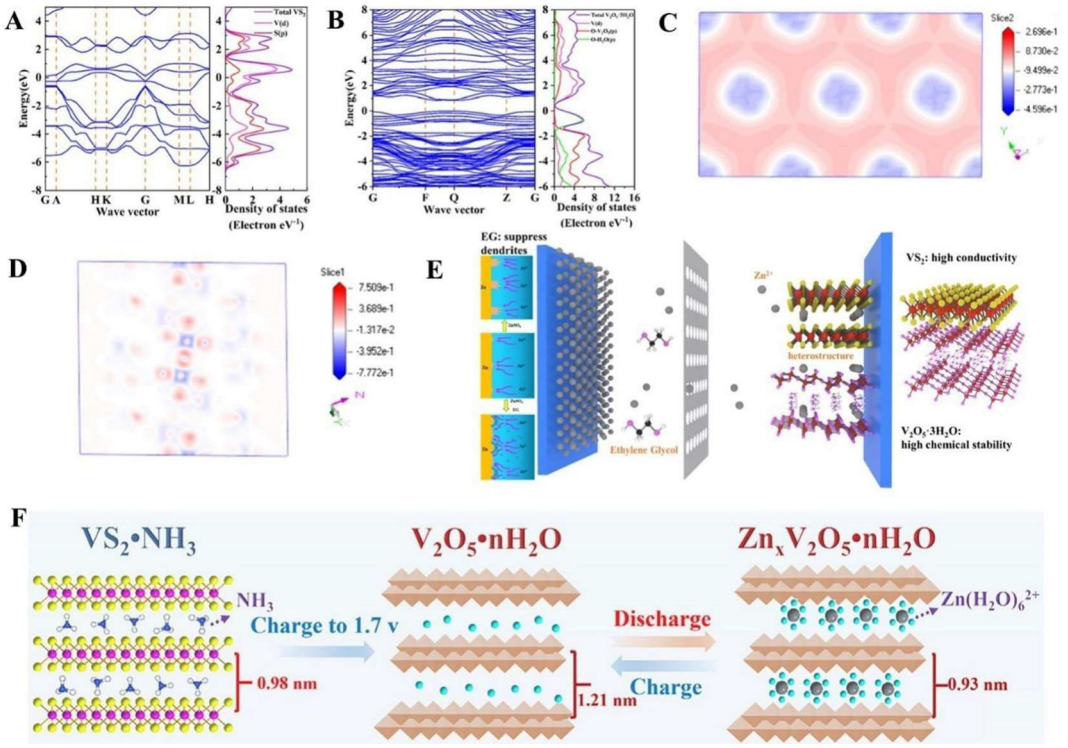

Figure 3 (A, B) Band structure and DOS plots of VS_2 and $V_2O_5 \cdot 3H_2O$. (C, D) Electron density differences of VS_2 and $V_2O_5 \cdot 3H_2O$. (E) Illustration of the charge/discharge process for the obtained aqueous ZIB. Reproduced with permission of Ref.[37], copyright 2022 American Chemical Society. (F) The electrochemical oxidation of $VS_2 \cdot NH_3$ process and the subsequent Zn^{2+} storage mechanism. Reproduced with permission of Ref.[38], copyright 2021 Elsevier. (color on line)

mAh·g^{-1}). Similar guideline can be made for sulfides, Liu et al.[36] prepared spindle-like VS_2 nanocrystals anchored onto N-doped carbon layer (VS_2@N-C) via *in-situ* hybridization. Results demonstrated that the strong interfacial interactions generated by the N-C composite significantly improved the charge transfer kinetics and cycle performance of the VS_2@N-C cathode. Hence, the VS_2@N-C//Zn ZIBs exhibited a high specific capacity of 203 mAh·g^{-1} at 0.05 mA·g^{-1} and a remarkable cycling stability of 97% of the initial capacity retention over 600 cycles at 1 A·g^{-1}.

In addition to compounding with highly conductive carbon materials, building heterostructures with other compounds is also an effective modification method. Yu et al.[20] synthesized a heterostructure VS_2/VO_x material by *in-situ* electrochemical strategy. Owing to the strong internal electric field at phase-boundary and the synergistic effect between the VS_2 with high electrical conductivity and the VO_x with high chemical stability, the heterostructure VS_2/VO_x cathode has obtained good electrochemical performance. Moreover, Gao et al.[37] also studied the synergistic effect of high conductive sulfides and high stability of oxides by constructing a biphasic V_2O_5·3H_2O@VS_2 nanocomposite. Owing to the lubricating effect of structural water in V_2O_5·3H_2O and the high conductivity of VS_2, proved by the first principles density functional theory (DFT) calculation (as demonstrated in Figure 3A-D), the V_2O_5·3H_2O@VS_2// Zn ZIBs showed excellent performances with high specific capacity (290 mAh·g^{-1} at 0.5 A·g^{-1}), improved rate capability (202 mAh·g^{-1} at 10 A·g^{-1}) and impressive long-term cycling life (69.7% capacity retention over 6700 cycles at 5 A·g^{-1}, with a reversible capacity of 207 mAh·g^{-1}).

In general, electrochemical oxidation has been regarded as a universal and facial strategy to boost the electrochemical performance of active materials with low-valence by forming new high-valence active materials[39-42]. Yang et al.[38] reported a flower-like VS_2·NH_3 hollow spheres cathode, which was further subjected to *in-situ* electrochemical oxidation (charged to 1.7 V) to obtain V_2O_5·nH_2O that actually participates in the reversible Zn^{2+} insertion/detachment process, and the electrochemical mechanisms are proposed based on *ex-situ* characterization, as shown in Figure 3F.

Moreover, defect engineering is widely used to regulate the electronic properties to improve the electrochemical performance. Yin et al.[43] prepared sulfur-deficient VS_2 (D-VS_2) as a AZIB cathode by defect engineering strategy. The DFT calculations demonstrated that Zn^{2+} ions are more prone to be stripped in the D-VS_2 than those in the pristine VS_2, promoting the electrochemical kinetics. As a result, the D-VS_2// Zn ZIBs exhibited a higher specific capacity (262 mAh·g^{-1} at 0.1 A·g^{-1}) than VS_2//Zn ZIBs (150 mAh·g^{-1} at 0.1 A·g^{-1}). Besides, VS_2//Zn ZIBs showed an enhanced cycling stability (94% capacity retention over 524 hours), which is superior to that of VS_2//Zn ZIBs (94% capacity retention over 270 hours).

2.2 VS_4 and Its Composites in AZIBs

As an equivalent of VS_2, VS_4 owns an intriguing one-dimensional (1D) atomic chain structure and has been widely investigated in recent years as a good intercalation cathode material for high performance AZIBs. It is worth noting that the anionic redox mechanism regarding conversion of original S_2^{2-} dimers to S^{2-} was detected in various types of VS_4-based ion batteries (Li^+/Na^+/Al^{3+}), which was expected to be an effective strategy to design cathodes with high energy density[44, 45]. Qin et al.[44] fabricated kernel like VS_4 particles immobilized on reduced graphene oxide (VS_4@rGO) by a one-step hydrothermal approach and proposed a possible energy storage mechanism involving coexistence of conversion reaction and Zn^{2+} insertion/extraction reaction by the *ex-situ* XPS testing, as shown in the following reactions:

Conversion mechanism:

$$2VS_4 + 11H_2O + 3Zn^{2+} \rightarrow Zn_3(OH)_2V_2O_7\cdot 2H_2O + 8S + 16H^+ + 10e^- \quad (4)$$

Intercalation mechanism:

$$VS_4 + xZn^{2+} + 2xe^- \leftrightarrow Zn_xVS_4 \quad (5)$$

Similarly, Gao et al.[46] prepared nano-flower like VS_4/carbon nanotubes (VS_4/CNTs) cathode with ex-

cellent Zn^{2+} storage capacity. In addition, the reaction mechanisms were further studied based on *ex-situ* characterizations to explain the unrepresentative nature of the first charge/discharge curves (Figure 4A and B). As presented in Figure 4D and E, the *ex-situ* XRD results showed that VS_4 underwent a phase transition process during the first discharge process (1.0 ~ 0.2 V), transforming into ZVO with an open framework structure accompanied by the formation of sulfur according to:

$$VS_4 + 11H_2O + 3Zn^{2+} + 6e^- \rightarrow Zn_3(OH)_2V_2O_7\cdot 2H_2O + 4S_2^{2-} + 8H^+ + 4H_2 \quad (6)$$

In the subsequent cycles, ZVO underwent a reversible Zn^{2+} insertion/extraction reaction. This phenomenon was also corroborated by *ex-situ* XPS measurement (Figure 4F). Thus, a mechanism involved phase change in the initial cycle and the reversible Zn^{2+} insertion/extraction of ZVO in subsequent cycles, is proposed for the VS_4, as shown in Figure 4G. Besides, the result of electrochemical dynamics sug-

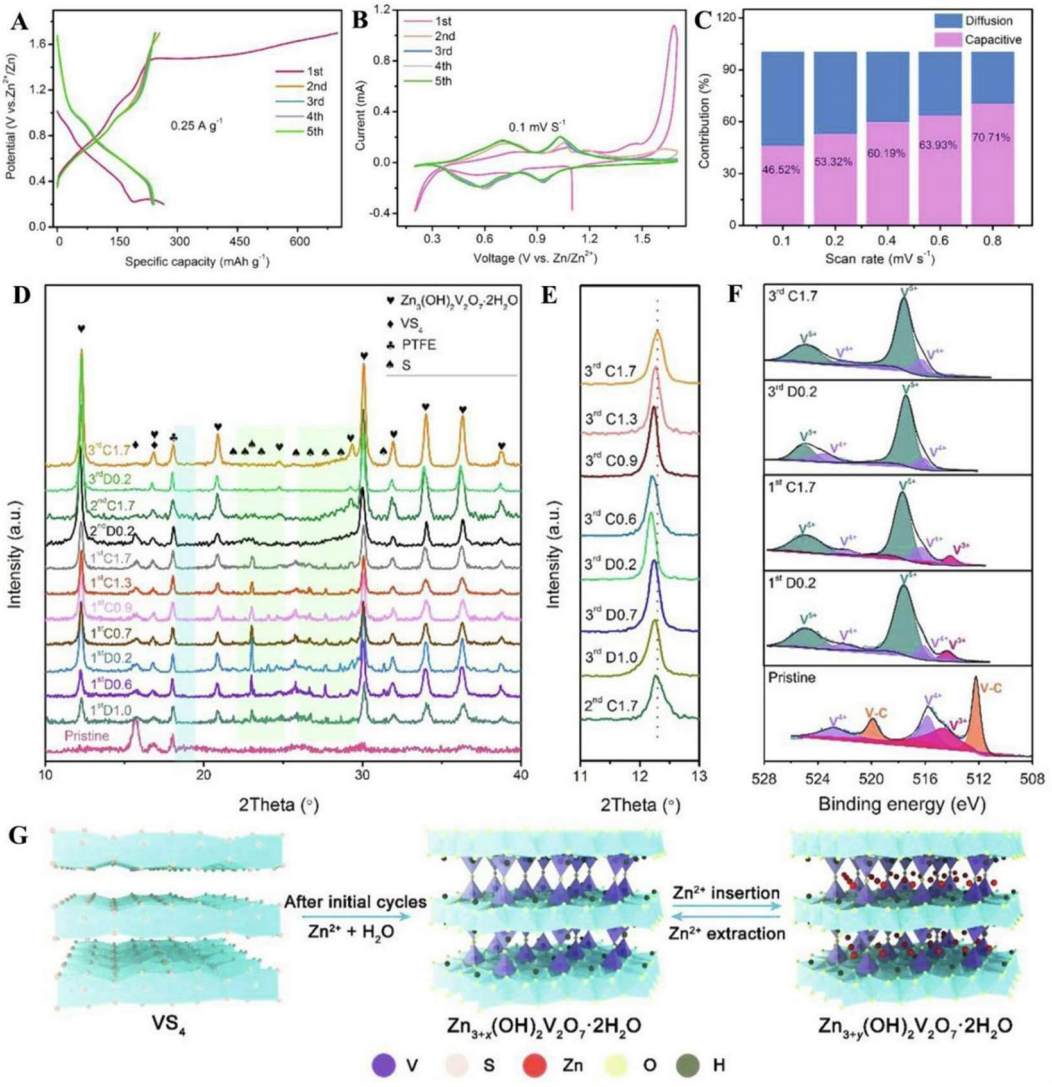

Figure 4 (A) Charge-discharge profiles of VS_4/CNTs at 0.25 A·g^{-1}. (B) CV curves at a scan rate of 0.1 mV·s^{-1}. (C) The capacitive and diffusion-controlled contributions of VS_4/CNTs electrode at different scan rates. (D) *Ex-situ* XRD patterns of cathode and (E) The enlarged area of ZVO (001) planes (11.5°~13.0°). (F) *Ex-situ* XPS spectra of V 2p. (G) Scheme showing the reaction mechanism of VS_4/CNTs electrode during cycling. Here $x<<y$. Reproduced with permission of Ref.[46], copyright 2021 Elsevier. (color on line)

gested that the ratio of capacitance contribution increases with the increasing scan rate, as shown in Figure 4C. Owing to the excellent Zn^{2+} diffusion co-efficient and wide ZVO plane spacing, the VS_4/CNTs cathode provided a reversible specific capacity of 265 mAh·g^{-1} at 0.25 A·g^{-1} and terrific cycle life with 93% of capacity retention over 1500 cycles at 5 A·g^{-1}.

On the basis of utilizing the conversion reaction to generate ZVO with large interlayer spacing, Samanta et al.[47] investigated a novel Mn-doped VS_4 (Mn-VS_4) as the AZIBs cathode. Mn doping can reduce the electron density around the V center (V^{4+}), which in turn transform to the VS_4 chain-like crystal phase, providing an open framework for the Zn^{2+} insertion/extraction. As a result, the Mn-VS_4 cathode exhibited an outstanding specific capacity (about 547 mAh·g^{-1} at 0.2 A·g^{-1}) and excellent cycling stability (97.83% of initial capacity retention over 1000 cycles at 1 A·g^{-1}). Combined with *ex-situ* characterizations (XRD, Field emission scanning electron microscope (FESEM), XPS, and Raman), the energy storage mechanism on coexistence of the conversion reaction and the reversible Zn^{2+} insertion/extraction reaction is also revealed, in consistent with that in previous research reported by Gao et al[46].

3 Vanadium Selenides and Their Composites

Vanadium diselenide (VSe_2) is a two-dimensional (2D) material with graphene like layered structure. It is arranged in a sandwich form of Se-V-Se with a large layer spacing (6.1 Å)[48, 49]. Moreover, it has excellent metal properties with the excellent conductivity (10^3 S·m^{-1}), which is greater than that of vanadium sulfide. Additionally, with low electronegativity, the energy barrier during ion intercalation or transport is largely reduced, all of which make VSe_2 a potential cathode for high performance AZIBs. Wang et al.[48] first applied layered VSe_2 with a large interlayer spacing in AZIBs and demonstrated the improved electrochemical performance. VSe_2//Zn AZIBs exhibited high specific reversible capacities of 250.6 and 132.6 mAh·g^{-1} at 0.2 and 5 A·g^{-1}, respectively, and superior cycle stability with 83% of initial capacity retention after 800 cycles at 2 A·g^{-1}. Furthermore, according to the *ex-situ* characterization, it was proposed that the reversible de/intercalation reaction in VSe_2 was responsible for the energy storage of Zn^{2+} ions:

$$VSe_2 + xZn^{2+} + 2xe^- \leftrightarrow Zn_xVSe_2. \quad (7)$$

Similarly, Wu et al.[49] prepared ultra-thin VSe_2 nanosheets with thickness of few layers by chemical liquid-phase synthesis, and verified the mechanisms of Zn^{2+} ions storage by *ex-situ* XRD and XPS characterizations, showing a two-step Zn^{2+} intercalation/deintercalation reactions (Figure 5A):

$$VSe_2 + 0.23Zn^{2+} + 0.46xe^- \leftrightarrow Zn_{0.23}VSe_2 \quad (8)$$

$$Zn_{0.23}VSe_2 + 0.17Zn^{2+} + 0.34e^- \leftrightarrow Zn_{0.4}VSe_2 \quad (9)$$

and the strong structure/crystal stability demonstrated by CV testing, capacity contribution calculations, and constant-current intermittent titration technique (GITT) analysis (Figure 5B-E). As manifested in Figure 5 F-J, the DFT calculation further revealed that VSe_2 nanosheets have strong metal properties and the optimal Zn^{2+} diffusion path, with a hopping energy barrier of 0.91 eV. The above results all indicated that ultra-thin VSe_2 nanosheets have great potential as cathode material for AZIBs.

Bai et al.[50] synthesized Se deficient VSe_2 nanosheets directly on a stainless steel (VSe_{2-x}-SS) cathode via one-step hydrothermal method. DFT calculations indicated that Se defects not only improved the conductivity, but also regulated the adsorption energy of Zn^{2+} ions, implying that the adsorption/desorption process of Zn^{2+} ions on VSe_{2-x}-SS cathode made better reversibility than that of VSe_2-SS cathode without the Se defects. Consequently, Zn//VSe_{2-x}-SS AZIBs exhibited a higher specific capacity (241.2 mAh·g^{-1} at 0.2 A·g^{-1}), better rate capability (230.1 mAh·g^{-1} at 4 A·g^{-1}), and more enhanced cycling stability (87.8% of initial capacity retention over 1800 cycles at 4 A·g^{-1}) than those of Zn//VSe_2-SS ZIBs. Furthermore, the energy storage mechanism (two-step intercalation process) for the VSe_{2-x}-SS cathode was investigated by *ex-situ* characterizations. The reaction process is

shown in Figure 5K, and the reactions can be expressed as:

$$VSe_{2-x}\text{-SS} + mZn^{2+} + 2me^- \leftrightarrow Zn_mVSe_{2-x}\text{-SS} \quad (10)$$

$$Zn_mVSe_{2-x}\text{-SS} + nZn^{2+} + 2ne^- \leftrightarrow Zn_m + nVSe_{2-x}\text{-SS} \quad (11)$$

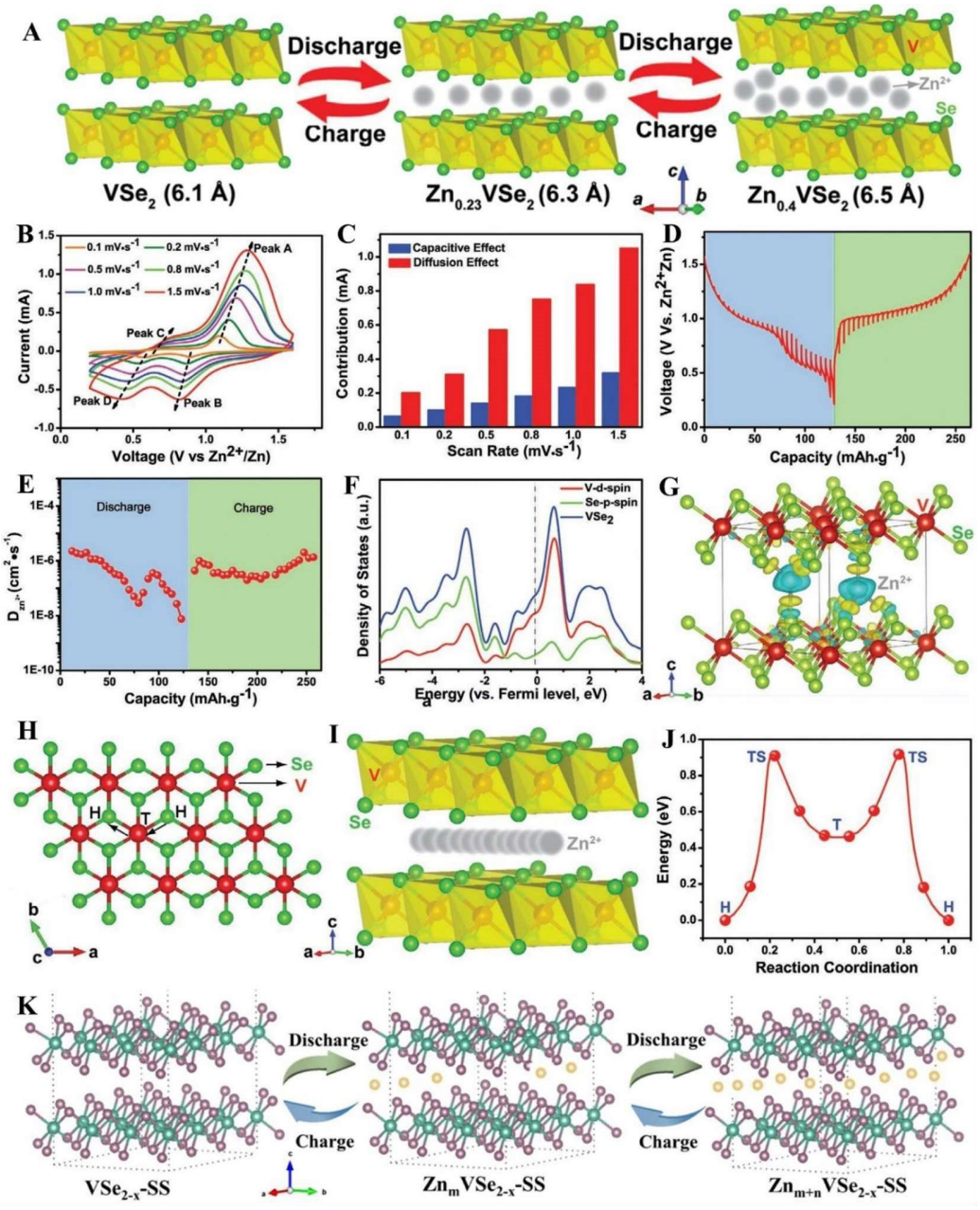

Figure 5 (A) Schematic illustration of the two-step Zn^{2+} intercalation/de-intercalation process in VSe_2 cathode. (B) CV curves of the Zn//VSe_2 battery at various scan rates. (C) The capacity contribution between capacitive effect and battery type. (D) GCD curve measured in GITT mode of the battery at the second cycle. (E) The calculated zinc-ion diffusion coefficient in the VSe_2 cathode at different charge/discharge stages. (F) Calculated partial spin-polarized projected density of states (DOS) for VSe_2. (G) Schematic illustration of charge density map after zinc-ion intercalation into the layered VSe_2 framework (yellow: charge increase; blue: charge decrease). (H) Top view and (I) side view of the optimal diffusion pathway of zinc ion. (J) Corresponding diffusion barrier curve based on the calculated diffusion pathway. Reproduced with permission of Ref.[49], copyright 2020 Wiley-VCH. (color on line) (K) Schematic diagram of the two-step Zn^{2+} insertion/extraction process for VSe_{2-x}-SS. Reproduced with permission of Ref.[50], copyright 2021 American Chemical Society. (color on line)

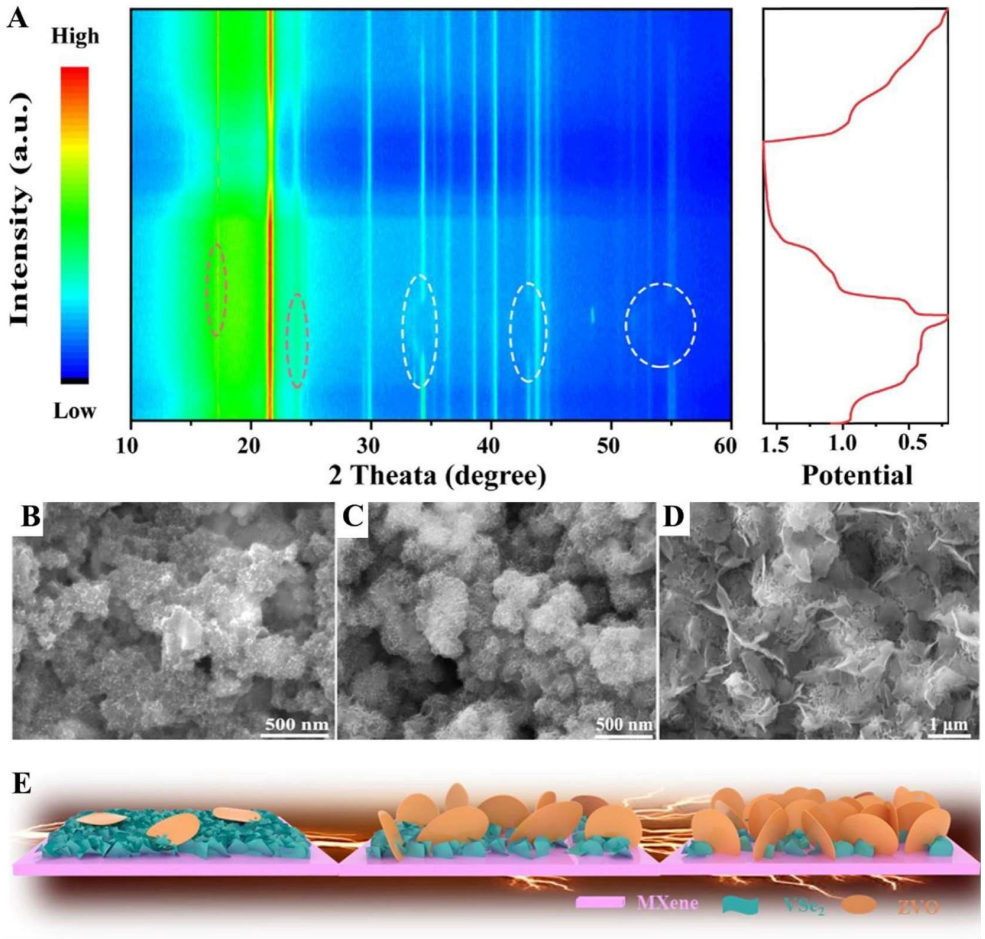

Figure 6 (A) *In-situ* XRD patterns of VSe_2/MXene electrode in the initial cycles against the voltage. (B-D) FESEM images for VSe_2/MXene electrode in 200, 500 and 2000 cycles. (E) Schematic diagram of electrode surface changing during long cycles. Reproduced with permission of Ref.[51], copyright 2022 Elsevier. (color on line)

Later, Cai et al.[51] prepared small-sized VSe_2 uniformly anchored on MXene (VSe_2/MXene). It was found that the VSe_2/MXene cathode exhibited an ever-increasing specific capacity during cycling, even after 1000 cycles. It was suggested that during the Zn^{2+}/H^+ interaction/extraction process, a significant oxidation reaction occurred under high voltages, and the formed vanadium oxide further reacts with Zn^{2+} in the electrolyte to form a new phase of $Zn_{0.25}V_2O_5 \cdot H_2O$ (PDF# 86-1238), as displayed in Figure 6A. Obviously, $Zn_{0.25}V_2O_5 \cdot H_2O$ was accumulated on the electrode surface as the number of cycles increased, which may be the reason for the continuous increase of specific capacity, as schematically shown in Figure 6B-E. This work provides a new understanding for the energy storage mechanism of AZIBs.

4 Vanadium Nitride and Its Composites for AZIBs

Vanadium nitride (VN) is an interstitial alloy compound in which vanadium atoms occupy a face center cube (FCC) lattice and nitrogen atoms fill in the octahedral interstices of metallic vanadium, forming a NaCl-type structure[52-54]. Therefore, VN has the characteristics of both covalent and ionic compounds, such as high melting point (2619 K), excellent hardness (1500 $kg \cdot mm^{-2}$), and outstanding electronic conductivity (10^6 $S \cdot m^{-1}$)[23, 42, 52]. In addition, owing to its good chemical stability, low molecular weight, high theoretical specific capacity, wide working voltage window, affordable price and abundant resources, VN has been extensively explored in the energy storage/conversion fields of catalysis, lithium ion batter-

ies and supercapacitors[55-57].

Since Ding et al.[42] first proposed that disordered rock salt vanadium oxynitride (VN_xO_y) has excellent Zn^{2+} ions storage capacity, researchers have increasingly paid their attention on VN as a cathode for AZIBs. Subsequently, Fang et al.[58] also fabricated a surface-oxidized vanadium nitride (VN_xO_y) cathode for AZIBs by a simple nitriding technique. The surface oxidation of VN_xO_y can improve the electrochemical activity, further promoting the electrochemical reaction kinetics. The co-existing reaction mechanisms of reversible interca lation (Zn^{2+}/H^+), redox reactions of cations (V^{3+}/V^{2+}), and reversible redox reactions of surface anions, significantly improved the performance of Zn//VN_xO AZIBs, delivering a high specific capacity of 240 mAh·g^{-1} at 1 A·g^{-1} and enhanced long-term cycling performance with a capacity retention of 75% after 2000 cycles at 20 A·g^{-1}.

Recently, tremendous efforts have been made to elucidate the energy storage mechanism of VN cathode in AZIBs. Bai et al. [23] fabricated ZnO quantum dots (QDs)-modified VN nanosheets (ZnO-QDs-VN) by a facile self-sacrificial template strategy. Compared with the original VN, ZnO-QDs-VN cathode exhibited

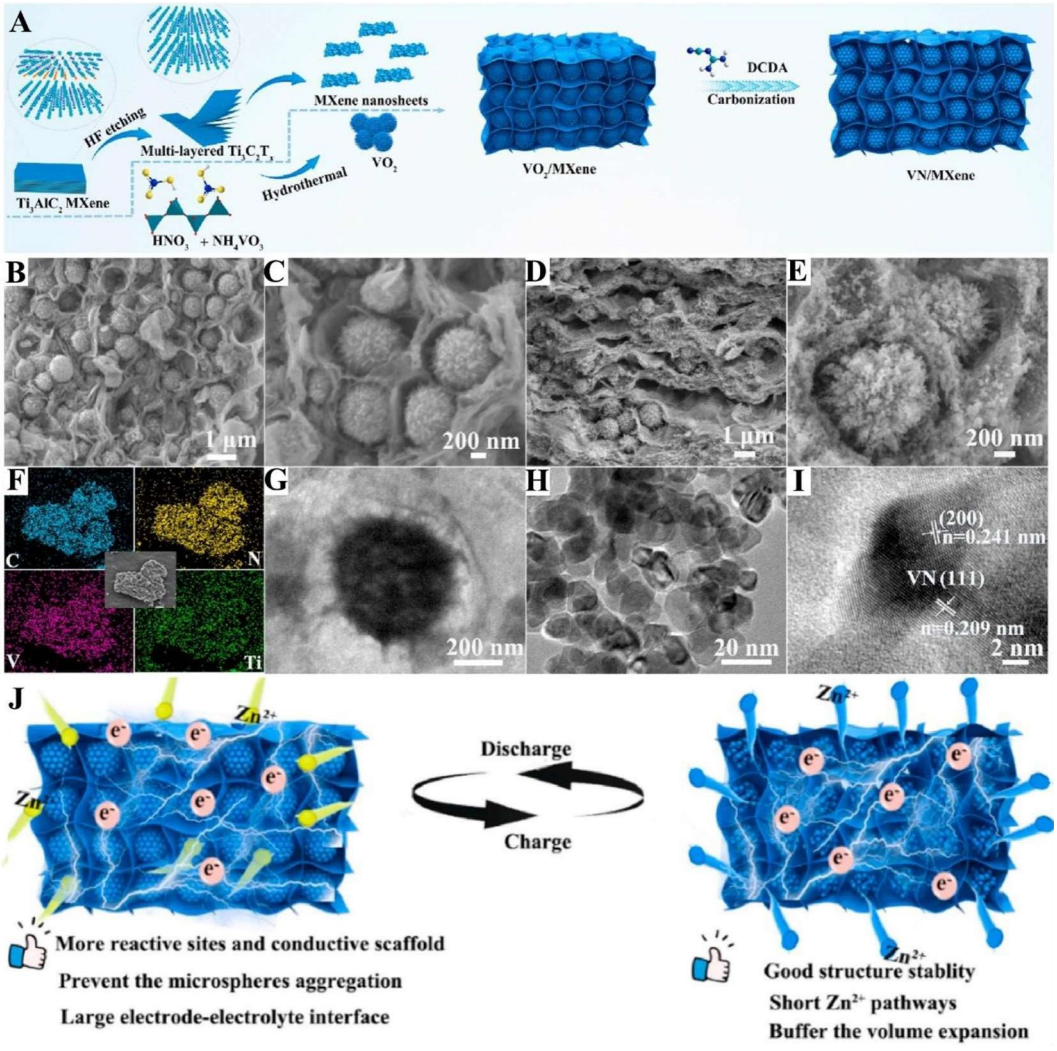

Figure 7 (A) Schematic illustration showing the formation process of 3D VN/MXene composite structure. (B, C) SEM images of VO_2/MXene. (D, E) SEM images, (F) EDS elemental mappings, (G, H) TEM images and (I) a HRTEM image of VN/MXene composite. (J) Schematic of VN/MXene electrodes during cycling. Reproduced with permission of Ref.[59], copyright 2022 Elsevier. (color on line)

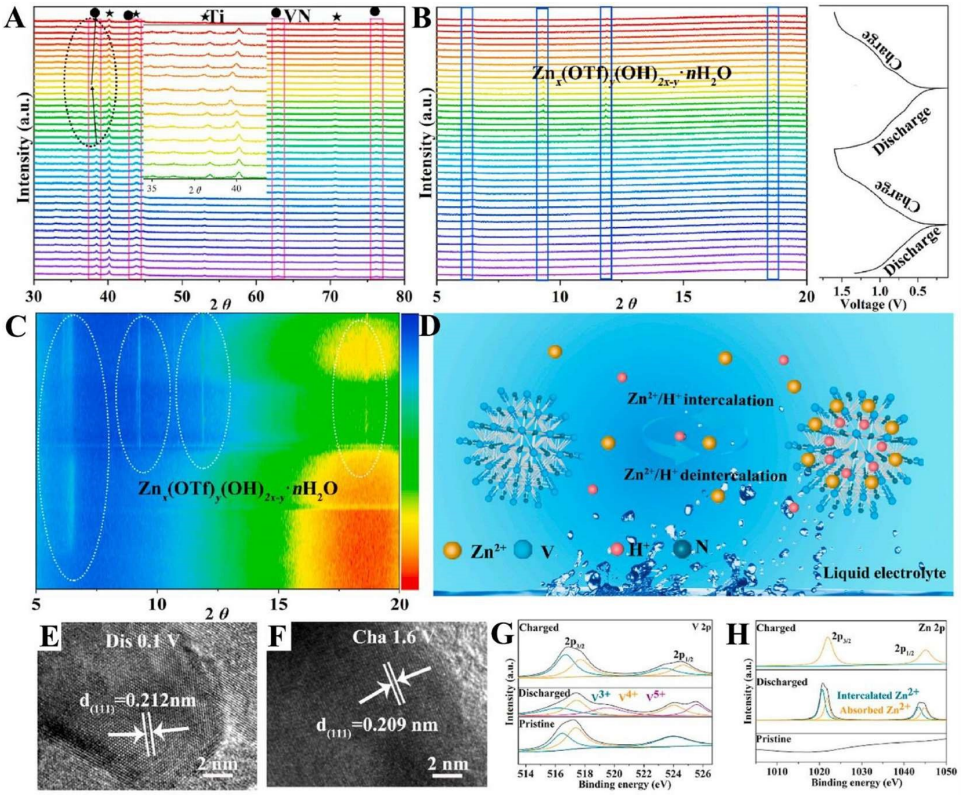

Figure 8 Zn-storage mechanism of VN. (A-C) *In-situ* XRD measurement in initial discharge/charge curve at 0.01 A·g^{-1} and the corresponding high-resolution contour maps between 5 ~ 20° and 30 ~ 80°, (E, F) HRTEM images of the fully discharged and charged electrode, (G, H) *Ex-situ* high-resolution XPS spectra of V 2p and Zn 2p at the fully discharged/charged state. (D) Schematic view of Zn^{2+} intercalation/de-intercalation in VN. Reproduced with permission of Ref.[59], copyright 2022 Elsevier. (color on line)

a highly enhanced specific capacity of 384.1 mAh·g^{-1} at 0.1 A·g^{-1} and extended cycle life with a capacity retention of about 60% over 1800 cycles at 5 A·g^{-1}. The results of *ex-situ* XRD pattern, high-resolution XPS and TEM characterizations all demonstrated the existence of the Zn^{2+} insertion/extraction mechanism, i.e., the electrochemical mechanism as follows:

$$VN + aZn^{2+} + 2ae^- \leftrightarrow Zn_bVN + Zn_{3+x}(OH)_{2+3x}V_{2-x}O_{7-3x}(H_2O)_2 \quad (12)$$

Later, Du et al.[59] encapsulated VN microspheres in an MXene matrix to construct a three-dimensional (3D) layered VN/MXene cathode, and the schematic illustration of the formation process is displayed in Figure 7A. The surface of the microspheres obtained after nitriding is relatively rough, providing abundant active sites for Zn^{2+} storage, and the morphology is shown in Figure 7B-I. Notably, combined with the tight coating of MXene, the agglomeration of VN microspheres is effectively avoided and the volume expansion during the charging/discharging process is greatly alleviated, leading to improving specific capacity and rate performance. Meanwhile, electrochemical mechanism of VN with reversible Zn^{2+}/H^+ co-insertion/extraction is proposed according to electrochemical results, and *in-situ* XRD/XPS and HRTEM analyses (Figures 8 A-C, E-H). Owing to the unique structure and co-intercalation mechanism (schematic as exhibited in Figure 8D), VN/MXene cathode achieved an excellent capacity of 521 mAh·g^{-1} at 0.5 A·g^{-1}, a long-term cycling stability with a capacity retention of 82.8% over 2000 cycles at 5 A·g^{-1}, and a high energy density of 478.1 Wh·kg^{-1}.

There is a view that low-valent vanadium nitride-based materials are prone to be oxidized to high-valence states, accompanied by obvious changes in physical and chemical properties, leading to enhanced

electrochemical performance. For the first time, Chen et al.[55] synthesized oxygen-doped vanadium nitride (O-VN) by annealing commercial vanadium pentoxide in ammonia, and proposed a new energy storage mechanism of cationic conversion reaction. Specifically, the phase transformation and morphologic evolution were comprehensively investigated using *ex-situ* XRD, SEM, and XPS characterizations. During charging process under weak acid conditions, the cathode underwent an O-VN → VO_2^+ → VO_x transition and then was reduced to V_2O_3 on the cathode surface during discharge. The V(III) species were subsequently oxidized back to cations dissolved into the electrolyte. Besides, the DFT calculations al so confirmed the reversibility of these reactions. benefiting from the mechanism of combined Zn^{2+} insertion/extraction with cation conversion reaction having more transferred ions, the O-VN cathode provided an ultra-high specific capacity of 705 mAh·g^{-1} at 0.2 A·g^{-1}. At current densities of 1.0 and 2.0 A·g^{-1}, the

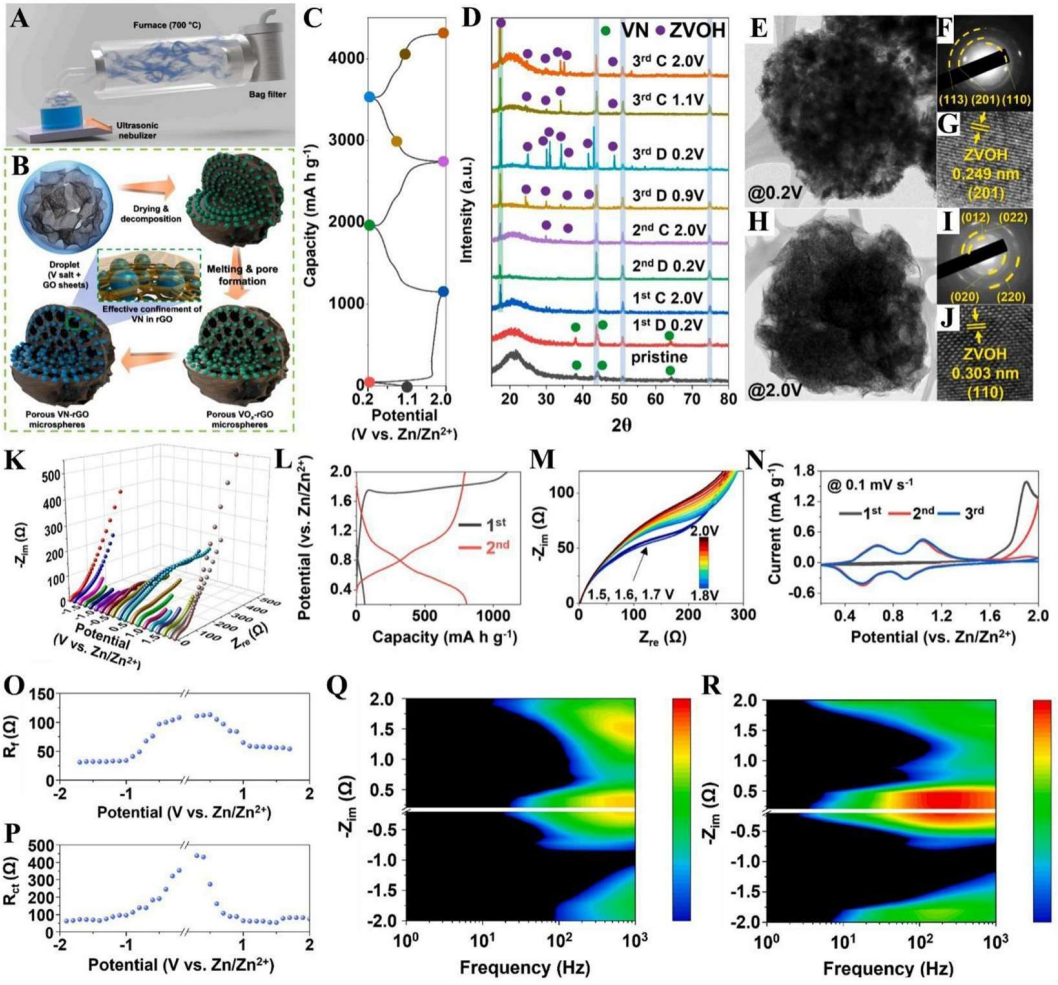

Figure 9 Schematic illustrations showing the spray pyrolysis apparatus (A) and formation mechanism of VN-rGO microspheres (B). (C) Galvanostatic charge-discharge profiles with dots indicating the selected potentials for *ex-situ* XRD measurements. (D) *Ex-situ* XRD patterns. *Ex-situ* TEM analysis for the (E-G) discharged and (H-J) charged states: (E, H) TEM images, (F, I) SAED patterns, and (G, J) HR-TEM images. (L) The 1st and 2nd charge/discharge profiles of VN-rGO microspheres at 0.1 A·g^{-1}, (M) *In-situ* EIS Nyquist plots obtained during initial charge process, (N) CV curves for the initial three cycles, *In-situ* EIS analysis: (K) Nyquist plots obtained at various potentials during the 3rd cycle, changes in (O) R_f and (P) R_{ct} as a function of potential. *In-situ* Bode plots for (Q) VN-rGO microspheres and (R) VN microspheres/rods. (the black region corresponds to phase angle < 45°). Reproduced with permission of Ref.[60], copyright 2022 Elsevier. (color on line)

O-VN cathode could provide specific capacities of 400 and 361 mAh·g^{-1} after 200 cycles, corresponding to capacity retentions of 60.5% and 57.5%, respectively. Some follow-up work has also been carried out on the exploration of the conversion reaction mechanism.

Since the composite of reduced graphene oxide (rGO) with the electrode materials can form a conductive network and provide a buffer layer to effectively alleviate the volume expansion, Chen et al.[61] prepared rGO-modified VN materials (VN@rGO) by electrostatic assembly way to improve the conductivity of VN. Moreover, electrochemical tests and kinetic studies demonstrated that the rGO accelerated the redox reaction on the electrode surface and improved the pseudocapacitive of the electrode by accelerating electron transfer. As a result, VN@rGO cathode exhibited a high specific capacity of 343 mAh·g^{-1} at 0.2 A·g^{-1}. Meanwhile, a ultra-long cycle stability with capacity retentions of 94.68% and 91.24% over 5851 A·g^{-1} and 10900 cycles at 20 A·g^{-1}, respectively, was achieved. In addition, *ex-situ* XRD, XPS and SEM characterizations were used to explore the energy storage mechanism of the electrode. The results revealed that VN was converted to $V_5O_{12}\cdot 6H_2O$ during the first charge (to 2.0 V), which became the host for Zn^{2+} insertion/extraction. It was also speculated that the activation process of the electrode was realized by the deposition/dissolution of $Zn_4SO_4(OH)_6\cdot 5H_2O$ to generate holes on the electrode surface. As a result, an energy storage mechanism combining conversion reaction and intercalation reaction is proposed:

First charge process (to 2.0 V):

$$5VN + 23H_2O \rightarrow V_5O_{12}\cdot 6H_2O + 5NH^{4+} + 5OH^- + 4.5H_2 \quad (13)$$

Intercalation reaction:

$$1.29Zn^{2+} + V_5O_{12}\cdot 6H_2O + 2.58e^- \leftrightarrow Zn_{1.29}V_5O_{12}\cdot 6H_2O \quad (14)$$

Similarly, Park et al.[60] prepared VN-rGO microspheres by spray pyrolysis and one-step nitrification, which is schematically illustrated in Figure 9A and B. The first three charge/discharge cycle curves are shown in Figure 9C. As presented in Figure 9D, the *ex-situ* XRD results showed that VN phase disappeared and a new phase of ZVO was formed in the first charging process. During the subsequent charge-discharge process, the peak intensity of the ZVO increased with discharging and decreased with the charging, implying the reversibility of Zn^{2+} insertion/extraction. The *ex-situ* TEM/HRTEM, SAED (Figure 9E-J) and XPS characterizations further demonstrated the above mechanism. Additionally, the *in-situ* EIS analysis was executed to further study the electrochemical reaction during charge-discharge process, as shown in Figure 9K-R. The EIS results present that VN-rGO, whether in the initial stage state or after the 100 cycles, exhibited smaller impendences than VN, indicating the superior Zn^{2+} ions diffusion kinetics in VN-rGO. As a result, the VN-rGO cathode exhibited an ultra-high specific capacity of 809 mAh·g^{-1} at 0.1 A·g^{-1}, a good rate performance with a reversible capability of 467 mAh·g^{-1} at 2 A·g^{-1}, and enhanced long-term cycling stability with a capacity retention of 78% after 400 cycles at 1 A·g^{-1}.

In general, VN has a high theoretical specific capacity as the cathode of AZIBs. However, in order to improve the practical capacity and enhance the cycle performance, it is necessary to adopt different methods to prepare a stable structural framework with unique morphology[62-64]. In addition, the energy storage mechanism of VN is complex and still controversial. In depth understanding of its energy storage mechanism is the pivotal to design novel cathodes for high-performance AZIBs.

5 Other Oxygen-Free Vanadium Compounds in AZIBs

In addition to the oxygen-free vanadium materials described above, a number of other oxygen-free vanadium materials have also been explored as cathodes in AZIBs. For instance, Li et al.[65] achieved direct transformation of MAX V_2AlC to V_2CT_x MXene within the battery using an F-rich electrolyte. The process was consisted of three main stages: stripping, oxidation of the electrode and redox of vanadium pentoxide. The V_2CT_x MXene exhibited a high specific capacity of 409.7 mAh·g^{-1} at 0.5 A·g^{-1} and an

exceptional rate performance of 97.5 mAh·g^{-1} even at current density as high as 64 A·g^{-1}. Later, Jiang et al.[25] synthesized S-doped modified V_2CT_x materials by molten salt method, and obtained good reversible specific capacity (411.3 mAh·g^{-1} at 0.5 A·g^{-1}) and an excellent cycling stability with 80% capacity retention after 3000 cycles at 10 A·g^{-1}.

In addition, the heterostructures obtained by partial oxidation of the oxygen-free vanadium-based MXene materials were also studied in AZIBs. For example, Venkatkarthick et al.[66] synthesized vanadium-based oxides on 2D vanadium carbide MXene (V_2O_x@V_2CT_x) by high-temperature etching and electrochemical cycling. As the ZIBs cathode, V_2O_x@V_2CT_x provided improved rate performance (304 and 84 mAh·g^{-1} at current densities 0.05 and 2 A·g^{-1}, respectively) and cycling performance (81.6% of initial capacity retention over 200 cycles at 1 A·g^{-1}) in 1 mol·L^{-1} $ZnSO_4$ electrolyte. Subsequently, Chen et al.[67] prepared VO_2@V_2C 1D/2D heterostructures by controlled oxidation of the V_2C surface via one-step hydrothermal method. VO_2@V_2C cathode also obtained excellent electrochemical performance. Furthermore, by selenizaiton of surface atoms of MXenes, Sha et al.[68] synthesized three transition metal selenides (VSe_2@V_2CT_x, $TiSe_2$@$Ti_3C_2T_x$ and $NbSe_2$@Nb_2CT_x) with high capacity and excellent structural stability. Among those three cathodes, VSe_2@V_2CT_x exhibited the highest rate capability (132.7 mAh·g^{-1} at 2.0 A·g^{-1}), and long-term cycling stability (93.1% capacity retention after 600 cycles at 2.0 A·g^{-1}). All of the above examples have inspired us to develop more novel oxygen-free vanadium materials in the future[23, 56, 69].

6 Summary and Outlooks

In this review, the development and application of oxygen-free vanadium compounds including vanadium sulfides, vanadium selenides, vanadium nitrides, other oxygen-free vanadium compounds, and their composites as cathodes in AZIBs are comprehensively summarized. Specifically, various design strategies, including morphological control, detect engineering, doping elements, composite construction with carbon materials or metal compounds, and direct growth of self-supporting cathodes without binder and conductive agent on the current collector, the electrochemical performance (Table 1), and the fundamental electrochemical mechanisms are emphasized. This review not only provides information about the recent development of oxygen-free vanadium compounds in AZIBs, but also sheds lights on design of novel high-performance cathodes for AZIBs, promoting the practical application of AZIBs.

Compared with other cathodes in AZIBs, the large interlayer spacing of vanadium-based materials is the key factor for their superior performance over other AZIBs cathode materials (namely, manganese-based oxides, Prussian blue analogs, and organic compounds). Intuitively, a detailed comparison in the various properties of AZIBs cathode materials is shown in Figure 10. The large interlayer spacing facilitates the diffusions of electrons/ions and Zn^{2+} insertion/extraction, thus promoting the diffusional kinetics of Zn^{2+}, and making it possess faster electrochemical kinetics. Combined with the high theoretical specific capacity, vanadium-based materials exhibit high energy density and power density after being converted into zinc ion batteries, which makes it stand out among many AZIBs cathode materials. Compared with vanadium-based oxides, oxygen-free vanadium compounds have emerged as novel cathodes for AZIBs and attracted increasing attention because of their higher electrical conductivity, larger layer spacing and lower ion diffusion barrier[81-83], exhibiting comparable or huger potential than vanadium-based oxides as cathodes for AZIBs.

Although great achievements have been made in oxygen-free vanadium compounds for AZIBs, further development of oxygen-free vanadium compounds still faces several similar challenges to these vanadium oxides[6, 84-86]. Challenges and possible solutions are proposed as following (Figure 11):

(1) Narrow working potential windows. Although vanadium-based compounds including oxygen-free vanadium compounds and vanadium oxides with layer structure have shown higher specific capacity, faster kinetics, and more enhanced long-term cycling

Table 1 Summary of electrochemical performance of oxygen-free vanadium-based materials as cathodes in ZIBs.

Material	Electrolyte	Voltage range/V	Specific capacity/mAh·g^{-1} (current density/ A·g^{-1})	Capacity retention (current density/ A·g^{-1}; cycles numbers)	Ref.
VS_2	1 mol·L^{-1} $ZnSO_4$	0.4 ~ 1.0	190.3 (0.05)	98% (0.5; 200)	[19]
VS_4@rGO	1 mol·L^{-1} $Zn(CF_3SO_3)_2$	0.35 ~ 1.8	180 (1.0)	93.3% (1; 165)	[44]
VS_2@SS	1 mol·L^{-1} $ZnSO_4$	0.4 ~ 1.0	198 (0.05)	80% (1; 1600)	[26]
VS_2@VOOH	3 mol·L^{-1} $ZnSO_4$	0.4 ~ 1.0	184.2 (0.05)	82% (2.5; 400)	[70]
D-VS_2	1 mol·L^{-1} $ZnSO_4$	0.2 ~ 1.7	262 (0.1)	94% (0.1; 100)	[43]
VS_2/VO_x	25 mol·L^{-1} $ZnCl_2$	0.1 ~ 1.8	301 (0.05)	75% (1; 3000)	[20]
VS_4	1 mol·L^{-1} $ZnSO_4$	0.2 ~ 1.6	310 (0.1)	-	[22]
VS_4/V_2O_3	3 mol·L^{-1} $Zn(CF_3SO_3)_2$	0.3 ~ 1.2	163 (0.1)	/	[71]
VS_2/CC	PVA-Zn/Mn hydrogel	0.4 ~ 1.0	175 (0.2)	~65% (0.2; 40)	[72]
VS_2@N-C	3 mol·L^{-1} $Zn(CF_3SO_3)_2$	0.2 ~ 1.8	203 (0.05)	97% (1; 600)	[36]
Mn-VS_4	1 mol·L^{-1} $Zn(OTf)_2$ ACN/water (1:1)	0.3 ~ 2.0	547 (0.2)	97.83% (1; 1000)	[47]
$V_2O_5·3H_2O$@VS_2	3 mol·L^{-1} $ZnSO_4$ EG/water (1:4)	0.3 ~ 1.6	290 (0.5)	69.7% (5; 6700)	[37]
VS_4/CNTs	2 mol·L^{-1} $Zn(CF_3SO_3)_2$	0.2 ~ 1.7	265 (0.25)	93% (5; 1200)	[46]
1T-VS_2	2.5 mol·L^{-1} $Zn(CF_3SO_3)_2$	0.4 ~ 0.85	212.9 (0.1)	86.7% (2; 2000)	[27]
VS_2	1 mol·L^{-1} $ZnSO_4$	0.2 ~ 1.0	450.7 (0.1)	72% (1; 200)	[73]
$VS_2·NH_3$	2 mol·L^{-1} $Zn(CF_3SO_3)_2$	0.2 ~ 1.7	392 (0.1)	110% (3; 2000)	[38]
VN_xO_y	2 mol·L^{-1} $ZnSO_4$	0.4 ~ 1.4	240 (1)	95% (1; 50) 75% (20; 2000)	[58]
ZnO-QDs-VN-	1 mol·L^{-1} $Zn(CF_3SO_3)_2$	0.4 ~ 1.6	384.1 (0.1)	~60% (5; 1800)	[23]
0.5O-VN	3 mol·L^{-1} $ZnSO_4$	0.2 ~ 2.0	705 (0.2)	60.5% (1; 200)	[55]
VN@rGO	3 mol·L^{-1} $ZnSO_4$	0.2 ~ 1.8	343 (0.2)	94.68% (1; 585) 91.24% (20; 10900)	[61]
VN	3.5 mol·L^{-1} $ZnSO_4$	0.2 ~ 1.8	496 (0.1)	53.6% (20; 8000)	[74]
VN/C	3.5 mol·L^{-1} $ZnSO_4$	0.2 ~ 1.8	321 (0.5)	76.6% (15; 6780) 95% (0.5; 720)	[75]
VN_xO_y/C	3 mol·L^{-1} $Zn(CF_3SO_3)_2$	0.2 ~ 1.6	407.4 (0.5)	93.4% (5; 2000)	[21]
VN@NGr	3 mol·L^{-1} $ZnSO_4$	0.2 ~ 1.8	~170 (0.5)	96.49% (0.1; 75) 70% (20; 26000)	[76]
VN/MXene	3 mol·L^{-1} $Zn(CF_3SO_3)_2$	0.1 ~ 1.6	521 (0.5)	82.8% (5; 2000)	[59]
VN/NC	3 mol·L^{-1} $Zn(CF_3SO_3)_2$	0.2 ~ 1.8	566 (0.2)	85% (10; 1000)	[57]
VN-rGO	1 mol·L^{-1} $Zn(CF_3SO_3)_2$	0.2 ~ 2.0	809 (0.1)	78% (1; 400)	[60]
VSe_2	2 mol·L^{-1} $ZnSO_4$	0.1 ~ 1.6	250.6 (0.2)	83% (2; 800)	[48]
VSe_2	2 mol·L^{-1} $ZnSO_4$	0.2 ~ 1.6	131.8 (0.1)	80.8% (1; 500)	[49]
VSe_{2-x}-SS	3 mol·L^{-1} $Zn(CF_3SO_3)_2$	0.4 ~ 1.6	241.2 (0.2)	87.8% (4; 1800)	[50]
rGO-VSe_2	2 mol·L^{-1} $ZnSO_4$	0.2 ~ 1.4	221.5 (0.5)	91.6% (0.5; 150)	[24]

Table 1 (Continued) Summary of electrochemical performance of oxygen-free vanadium-based materials as cathodes in ZIBs.

Material	Electrolyte	Voltage range/V	Specific capacity/mAh·g^{-1} (current density/ A·g^{-1})	Capacity retention (current density/ A·g^{-1}; cycles numbers)	Ref.
V_2O_5@V_2C	2.5 mol·L^{-1} $ZnSO_4$	0.2 ~ 1.4	397 (0.5)	87% (4; 2000)	[77]
VO_2@V_2C	3 mol·L^{-1} $Zn(CF_3SO_3)_2$	0.2 ~ 1.2	456 (0.2)	81% (5; 1000)	[67]
NVGO	6 mol·L^{-1} KOH	1.2 ~ 2.1	253.9 (0.5)	70% (4.5; 500)	[78]
V_2CT_x	3 mol·L^{-1} $ZnSO_4$+1 mol·L^{-1} Li_2SO_4	0.25 ~ 1.6	423 (1.0)	~94% (30; 2000)	[79]
V_2O_5@V_2CT_x	1 mol·L^{-1} $ZnSO_4$	0.2 ~ 1.6	304 (0.05)	81.6% (1; 200)	[66]
K-V_2C@MnO_2	2 mol·L^{-1} $ZnSO_4$+0.25 mol·L^{-1} $MnSO_4$	0.8 ~ 1.8	408.1 (0.3)	＞100% (10; 10000)	[80]
MS-S-V_2CT_x	2 mol·L^{-1} $ZnSO_4$	0.2 ~ 1.8	411.3 (0.5)	80% (10; 3000)	[25]
VSe_2@V_2CT_x	2 mol·L^{-1} $Zn(CF_3SO_3)_2$	0.0 ~ 1.6	302.1 (0.1)	93.1% (2; 600)	[68]

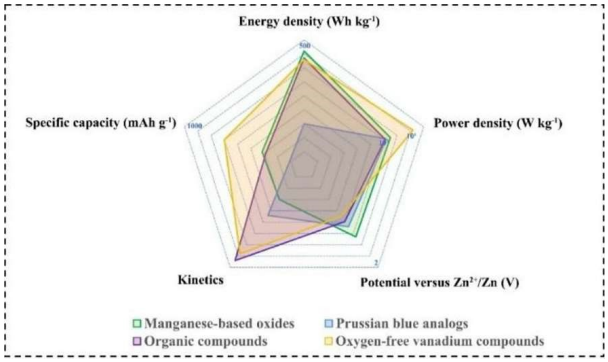

Figure 10 Comparison in different kinds of cathode materials for AZIBs (color on line)

stability than other cathodes such as manganese oxides, Prussian blue analogs, and organic compounds in AZIBs, the narrow average potential (≤ 1 V) severely lowers their energy density. Designing vanadium-based compounds with both high specific capacity and large working potential is imperative, though challenging, to construct high-performance AZIBs with high energy density.

(2) Moreover, oxygen-free vanadium compounds also have some common scientific problems of vanadium-based materials, such as the dissolution of vanadium in electrolyte, electrostatic interaction between Zn^{2+} and host skeleton, poor conductivity, and severe side reactions during circulation, which still need continuous attention and find resolution in the future. These problems can generally be effectively suppressed by pre-addition of relevant salts, pre-insertion of metal ions/structural water, nanostructures and oxygen vacancy construction, composite of highly conductive materials and modification of Zn anode alloying. In the future studies, how to improve the electrochemical properties of AZIBs based on oxygen-free vanadium by optimizing the structure of cathode materials and preparing stable electrode materials remains to be explored.

(3) "Structure-property" relationship in vanadium-based compounds is unclear. More sophisticated strategies are needed to design high-performance oxygen-free vanadium compounds. As the research of oxygen-free vanadium compounds is still in its infancy, design strategies adopted to prepare novel cathodes are limited. Some effective design methods in vanadium-based oxides have not been applied to oxygen-free vanadium compounds, such as insertion of metal ions and adjustment of structural water[12, 48, 87-89]. Referring to the design strategies in vanadium-based oxides or other cathodes that have been extensively studied may bring into great breakthrough in oxygen-free vanadium-based compounds.

(4) The zinc storage mechanisms in vanadium-based cathodes remain controversial. Exploration of zinc storage mechanisms is important for the fundamental understanding for electrode design. Generally speaking, the energy storage mechanism in aqueous solution

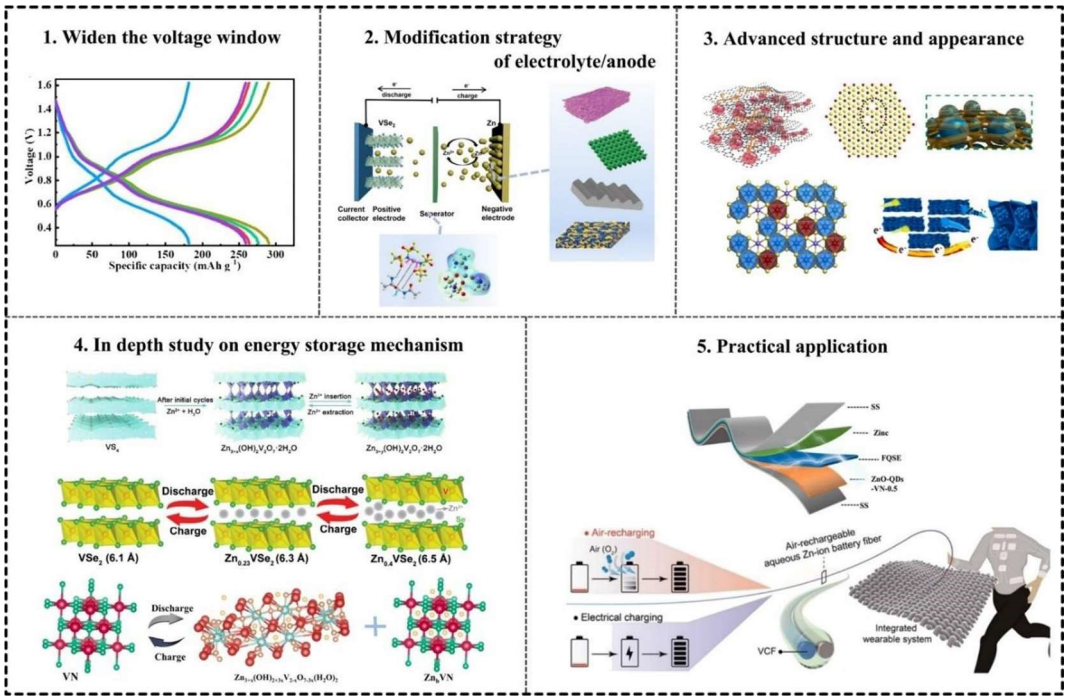

Figure 11 Outlooks to the development of oxygen-free vanadium compounds for AZIBs (color on line)

is complex. While researches have been conducted to explore the corresponding energy storage mechanisms for oxygen-free vanadium compounds cathode, an undisputed mechanism is hard to be achieved up to now[48, 58]. With the help of *in-situ*/*ex-situ* characterization techniques, the traditional Zn^{2+} interpolation/deintercalation mechanism, Zn^{2+}/H^+ co-insertion mechanism, two-step intercalation reaction mechanism and novel redox conversion mechanism have been proposed successively[73, 90]. Understanding the microstructural evolution and reaction mechanisms is beneficial to providing theoretical guidance for the rational design and application of aqueous solutions in the future. Due to the lack of a comprehensive, detailed theoretical basis and advanced standard characterization techniques, the Zn storage mechanism of oxygen-free vanadium compounds remains difficult to be clearly explained. Therefore, the development of more accurate characterization technology (such as *in-situ*/*operando* techniques), combined with advanced theoretical calculation is imperative to understand the storage mechanism of Zn and the relationship between structure and property[12, 88, 91, 92].

(5) The practical issues of oxygen-free vanadium-based cathodes for the commercialization of AZIBs. In order to meet the increasing demand of high-performance AZIBs with high energy density, one should not only take into consideration of the parameters such as specific capacity, long-term cycling stability, and rate performance, other factors such as loading of electrode, capacity ratio of negative to positive electrodes (N/P), and the amount of electrolytes are also paramount important to achieve high-performance with satisfying energy density[63, 93, 94]. However, the recent research only focuses on specific capacity and cycling performance without mention of the loading of active materials. Actually, it is well accepted that the specific capacity and cycling performance are also tightly related with the loading of active materials, N/P, and electrolyte amount. Moreover, compared with lithium-ion batteries, AZIBs are more suitable for flexible and wearable electronics due to their intrinsic safety[95, 96]. Therefore, design binder-free oxygen-free vanadium-based compounds with excellent flexibility is a facile strategy to construct flexible AZIBs for future application.

Conflicts of interest

There are no conflicts to declare.

Acknowledgements

This work was supported by Seed Fund of National University of Defense Technology.

References:

[1] Park S K, Dose W M, Boruah B D, De Volder M. *In situ* and operando analyses of reaction mechanisms in vanadium oxides for Li-, Na-, Zn-, and Mg- ions batteries[J]. Adv. Mater. Technol., 2021, 7(1): 2100799.

[2] Yi T F, Qiu L Y, Qu J P, Liu H Y, Zhang J H, Zhu Y R. Towards high-performance cathodes: Design and energy storage mechanism of vanadium oxides-based materials for aqueous Zn-ion batteries[J]. Coordin. Chem. Rev., 2021, 446: 214124.

[3] Li X R, Cheng H Y, Hu H, Pan K M, Yuan T T, Xia W T. Recent advances of vanadium-based cathode materials for zinc-ion batteries[J]. Chinese Chem. Lett., 2021, 32(12): 3753-3761.

[4] Zhou T, Han Q, Xie L L, Yang X L, Zhu L M, Cao X Y. Recent developments and challenges of vanadium oxides (V_xO_y) cathodes for aqueous zinc-ion batteries[J]. Chem. Rec., 2022, 22(4): e202100275.

[5] Du M, Miao Z Y, Li H Z, Sang Y H, Liu H, Wang S H. Strategies of structural and defect engineering for high-performance rechargeable aqueous zinc-ion batteries [J]. J. Mater. Chem. A, 2021, 9(35): 19245-19281.

[6] Wang H Y, Ye W Q, Yang Y, Zhong Y J, Hu Y. Zn-ion hybrid supercapacitors: Achievements, challenges and future perspectives[J]. Nano Energy, 2021, 85: 105942.

[7] Wang X, Zhang Z C Y, Xi B J, Chen W H, Jia Y X, Feng J K, Xiong S L. Advances and perspectives of cathode storage chemistry in aqueous zinc-ion batteries[J]. ACS Nano, 2021, 15(6): 9244-9272.

[8] Cai K X, Luo S H, Feng J, Wang J C, Zhan Y, Wang Q, Zhang Y H, Liu X. Recent advances on spinel zinc manganate cathode materials for zinc-ion batteries[J]. Chem. Rec., 2022, 22(1): e202100169.

[9] Zhang N, Chen X Y, Yu M, Niu Z Q, Cheng F Y, Chen J. Materials chemistry for rechargeable zinc-ion batteries[J]. Chem. Soc. Rev., 2020, 49(13): 4203-4219.

[10] Liu S, Kang L, Kim J M, Chun Y T, Zhang J, Jun S C. Recent advances in vanadium-based aqueous rechargeable zinc-ion batteries[J]. Adv. Energy Mater., 2020, 10(25): 2000477.

[11] Mathew V, Sambandam B, Kim S, Kim S, Park S, Lee S, Alfaruqi M H, Soundharrajan V, Islam S, Putro D Y, Hwang J Y, Sun Y K, Kim J. Manganese and vanadium oxide cathodes for aqueous rechargeable zinc-ion batteries: A focused view on performance, mechanism, and developments[J]. ACS Energy Lett., 2020, 5(7): 2376-2400.

[12] Wan F, Niu Z Q. Design strategies for vanadium-based aqueous zinc-ion batteries[J]. Angew. Chem. Int. Ed., 2019, 58(46): 16358-16367.

[13] Li Y, Zhang D H, Huang S Z, Yang H Y. Guest-species-incorporation in manganese/vanadium-based oxides: Towards high performance aqueous zinc-ion batteries [J]. Nano Energy, 2021, 85: 105969.

[14] Li H F, Ma L T, Han C P, Wang Z F, Liu Z X, Tang Z J, Zhi C Y. Advanced rechargeable zinc-based batteries: Recent progress and future perspectives[J]. Nano Energy, 2019, 62: 550-587.

[15] Xu W W, Wang Y. Recent progress on zinc-ion rechargeable batteries[J]. Nanomicro. Lett., 2019, 11(1): 90.

[16] Li C, Chen Y F, Zhang J, Jiang H L, Zhu Y H, Jia J H, Bai S X, Fang G Z, Zheng C M. MOF-derived porous carbon inlaid with MnO_2 nanoparticles as stable aqueous Zn-ion battery cathodes[J]. Dalton Trans., 2021, 50(47): 17723-17733.

[17] Li C, Zheng C M, Jiang H L, Bai S X, Jia J H. Conductive flower-like Ni-PTA-Mn as cathode for aqueous zinc-ion batteries[J]. J. Alloy. Compd., 2021, 882: 160587.

[18] Ding J W, Gao H G, Ji D F, Zhao K, Wang S W, Cheng F Y. Vanadium-based cathodes for aqueous zinc-ion batteries: From crystal structures, diffusion channels to storage mechanisms[J]. J. Mater. Chem. A, 2021, 9(9): 5258-5275.

[19] He P, Yan M Y, Zhang G B, Sun R M, Chen L N, An Q Y, Mai L Q. Layered VS_2 nanosheet-based aqueous Zn ion battery cathode[J]. Adv. Energy Mater., 2017, 7(11): 1601920.

[20] Yu D X, Wei Z X, Zhang X Y, Zeng Y, Wang C Z, Chen G, Shen Z X, Du F. Boosting Zn^{2+} and NH_4^+ storage in aqueous media via *in-situ* electrochemical induced VS_2/VO_x heterostructures[J]. Adv. Funct. Mater., 2020, 31(11): 2008743.

[21] Yang H L, Ning P G, Wen J W, Xie Y B, Su C L, Li Y P, Cao H B. Structure control in VN_xO_y by hydrogen bond association extraction for enhanced zinc ion storage [J]. Electrochimi. Acta, 2021, 389: 138722.

[22] Zhu Q C, Xiao Q, Zhang B W, Yan Z C, Liu X, Chen S, Ren Z F, Yu Y. VS_4 with a chain crystal structure used as an intercalation cathode for aqueous Zn-ion batteries [J]. J. Mater. Chem. A, 2020, 8(21): 10761-10766.

[23] Bai Y C, Zhang H, Xiang B, Yao Q, Dou L, Dong G Y. Engineering porous structure in bi-component-active ZnO quantum dots anchored vanadium nitride boosts reaction kinetics for zinc storage[J]. Nano Energy, 2021, 89: 106386.

[24] Narayanasamy M, Hu L T, Kirubasankar B, Liu Z T, Angaiah S, Yan C. Nanohybrid engineering of the vertically confined marigold structure of rGO-VSe_2 as an advanced cathode material for aqueous zinc-ion battery[J]. J. Alloys and Compd., 2021, 882: 160704.

[25] Jiang W Y, Shi H Z, Shen M, Tang R, Tang Z F, Wang J Q. Molten salt thermal treatment synthesis of S-doped V_2CT_x and its performance as a cathode in aqueous Zn-ion batteries[J]. ACS Appl. Mater. Interfaces, 2022, 14(12): 14482-14491.

[26] Jiao T P, Yang Q, Wu S L, Wang Z F, Chen D, Shen D, Liu B, Cheng J Y, Li H F, Ma L T, Zhi C Y, Zhang W J. Binder-free hierarchical VS_2 electrodes for high-performance aqueous Zn ion batteries towards commercial level mass loading[J]. J. Mater. Chem. A, 2019, 7(27): 16330-16338.

[27] Tan Y, Li S W, Zhao X D, Wang Y, Shen Q Y, Qu X H, Liu Y C, Jiao L F. Unexpected role of the interlayer "dead Zn^{2+}" in strengthening the nanostructures of VS_2 cathodes for high-performance aqueous Zn-ion storage [J]. Adv. Energy Mater., 2022, 12(19): 2104001.

[28] Dong L B, Yang W, Yang W, Li Y, Wu W J, Wang G X. Multivalent metal ion hybrid capacitors: A review with a focus on zinc-ion hybrid capacitors[J]. J. Mater. Chem. A, 2019, 7(23): 13810-13832.

[29] Yu P, Zeng Y X, Zhang H Z, Yu M H, Tong Y X, Lu X H. Flexible Zn-ion batteries: Recent progresses and challenges[J]. Small, 2019, 15(7): 1804760.

[30] Wang X, Li Y G, Wang S, Zhou F, Das P, Sun C L, Zheng S H, Wu Z S. 2D amorphous V_2O_5/graphene heterostructures for high-safety aqueous Zn-ion batteries with unprecedented capacity and ultrahigh rate capability [J]. Adv. Energy Mater., 2020, 10(22): 2000081.

[31] Yan M Y, He P, Chen Y, Wang S Y, Wei Q L, Zhao K N, Xu X, An Q Y, Shuang Y, Shao Y Y, Mueller K T, Mai L Q, Liu J, Yang J H. Water-lubricated intercalation in $V_2O_5\cdot nH_2O$ for high-capacity and high-rate aqueous rechargeable zinc batteries[J]. Adv. Mater., 2018, 30(1), 1703725.

[32] Dai X, Wan F, Zhang L L, Cao H M, Niu Z Q. Freestanding graphene/VO_2 composite films for highly stable aqueous Zn-ion batteries with superior rate performance [J]. Energy Storage Mater., 2019, 17: 143-150.

[33] Pang Q, Sun C L, Yu Y H, Zhao K N, Zhang Z Y, Voyles P M, Chen G, Wei Y J, Wang X D. $H_2V_3O_8$ nanowire/graphene electrodes for aqueous rechargeable zinc ion batteries with high rate capability and large capacity[J]. Adv. Energy Mater., 2018, 8(19): 1800144.

[34] Hu P, Zhu T, Wang X P, Zhou X F, Wei X J, Yao X H, Luo W, Shi C W, Owusu K A, Zhou L, Mai L Q. Aqueous Zn//Zn$(CF_3SO_3)_2$/$Na_3V_2(PO_4)_3$ batteries with simultaneous Zn^{2+}/Na^+ intercalation/de-intercalation[J]. Nano Energy, 2019, 58: 492-498.

[35] Li C, Zheng C M, Jiang H L, Bai S X, Jia J H. Synergistic effect of structural stability and oxygen vacancies enabling long-life aqueous zinc-ion battery[J]. Mater Lett., 2021, 302: 130373.

[36] Liu J P, Peng W C, Li Y, Zhang F B, Fan X B. A VS_2@N-doped carbon hybrid with strong interfacial interaction for high-performance rechargeable aqueous Zn-ion batteries[J]. J. Mater. Chem. C, 2021, 9(19): 6308-6315.

[37] Gao P, Pan Z K, Ru Q, Zhang J, Zheng M H, Zhao X, Ling F C C, Wei L. Synergetic $V_2O_5\cdot 3H_2O$/metallic VS_2 nanocomposites endow a long life and high rate capability to aqueous zinc-ion batteries[J]. Energy Fuel., 2022, 36(6): 3319-3327.

[38] Yang M Y, Wang Z F, Ben H Y, Zhao M X, Luo J X, Chen D Z, Lu Z G, Wang L, Liu C. Boosting the zinc ion storage capacity and cycling stability of interlayer-expanded vanadium disulfide through *in-situ* electrochemical oxidation strategy[J]. J. Colloid. Interface Sci., 2022, 607: 68-75.

[39] Cao Z Y, Chu H, Zhang H, Ge Y C, Clemente R, Dong P, Wang L P, Shen J F, Ye M X, Ajayan P M. An *in situ* electrochemical oxidation strategy for formation of nanogrid-shaped $V_3O_7\cdot H_2O$ with enhanced zinc storage properties[J]. J. Mater. Chem. A, 2019, 7(44): 25262-25267.

[40] Wang J J, Wang J G, Liu H Y, You Z Y, Wei C G, Kang F Y. Electrochemical activation of commercial MnO microsized particles for high-performance aqueous zinc-ion batteries[J]. J. Power Sources, 2019, 438: 226951.

[41] Ding J W, Gao H G, Zhao K, Zheng H Y, Zhang H, Han L F, Wang S W, Wu S D, Fang S M, Cheng F Y. *In-situ* electrochemical conversion of vanadium dioxide for enhanced zinc-ion storage with large voltage range[J]. J. Power Sources, 2021, 487: 229369.

[42] Ding J W, Du Z G, Li B, Wang L Z, Wang S W, Gong Y J, Yang S B. Unlocking the potential of disordered rocksalts for aqueous zinc-ion batteries[J]. Adv. Mater., 2019, 31(44): 1904369.

[43] Yin B S, Zhang S W, Xiong T, Shi W, Ke K, Lee W S V, Xue J M, Wang Z B. Engineering sulphur vacancy in VS_2 as high performing zinc-ion batteries with high cyclic stability[J]. New J Chem., 2020, 44(37): 15951-15957.

[44] Qin H G, Yang Z H, Chen L L, Chen X, Wang L M. A high-rate aqueous rechargeable zinc ion battery based on the VS_4@rGO nanocomposite[J]. J. Mater. Chem. A, 2018, 6(46): 23757-23765.

[45] Liu S N, Chen X X, Zhang Q, Zhou J, Cai Z Y, Pan A Q. Fabrication of an inexpensive hydrophilic bridge on a carbon substrate and loading vanadium sulfides for flexible aqueous zinc-ion batteries[J]. ACS Appl. Mater. Inter., 2019, 11(40): 36676-36684.

[46] Gao S Z, Ju P, Liu Z Q, Zhai L, Liu W B, Zhang X Y, Zhou Y L, Dong C F, Jiang F Y, Sun J C. Electrochemically induced phase transition in a nanoflower vanadium tetrasulfide cathode for high-performance zinc-ion batteries[J]. J. Energy Chem., 2022, 69: 356-362.

[47] Samanta P, Ghosh S, Jang W, Yang C M, Murmu N C, Kuila T. A reversible anodizing strategy in a hybrid electrolyte Zn-ion battery through structural modification of a vanadium sulfide cathode[J]. ACS Appl. Energ. Mater., 2021, 4(10): 10656-10667.

[48] Wang L L, Wu Z X, Jiang M J H, Lu J Y, Huang Q H, Zhang Y, Fu L J, Wu M, Wu Y P. Layered VSe_2: A promising host for fast zinc storage and its working mechanism[J]. J. Mater. Chem. A, 2020, 8(18): 9313-9321.

[49] Wu Z Y, Lu C J, Wang Y N, Zhang L, Jiang L, Tian W C, Cai C L, Gu Q F, Sun Z M, Hu L F. Ultrathin VSe_2 nanosheets with fast ion diffusion and robust structural stability for rechargeable zinc-ion battery cathode[J]. Small, 2020, 16(35): 2000698.

[50] Bai Y C, Zhang H, Xiang B, Liang X Y, Hao J Y, Zhu C, Yan L J. Selenium defect boosted electrochemical performance of binder-free VSe_2 nanosheets for aqueous zinc-ion batteries[J]. ACS Appl. Mater. Interfaces, 2021, 13(19): 23230-23238.

[51] Cai S N, Wu Y K, Chen H, Ma Y D, Fan T X, Xu M W, Bao S J. Why does the capacity of vanadium selenide based aqueous zinc ion batteries continue to increase during long cycles?[J]. J. Colloid. Interface Sci., 2022, 615: 30-37.

[52] Fechler N, Tiruye G A, Marcilla R, Antonietti M. Vanadium nitride@N-doped carbon nanocomposites: Tuning of pore structure and particle size through salt templating and its influence on supercapacitance in ionic liquid media[J]. RSC Adv., 2014, 4(51): 26981-26989.

[53] Yuan J, Hu X, Chen J X, Liu Y J, Huang T Z, Wen Z H. *In situ* formation of vanadium nitride quantum dots on N-doped carbon hollow spheres for superior lithium and sodium storage[J]. J. Mater. Chem. A, 2019, 7(15): 9289-9296.

[54] Ou L N, Liu Z X, Zhou Y F, Ou H H, Zhu J, Cao X X, Fang G Z, Zhou J, Liang S Q. Pseudocapacitance-dominated zinc storage enabled by nitrogen-doped carbon stabilized amorphous vanadyl phosphate[J]. Chem. Eng. J., 2021, 426: 131868.

[55] Chen D, Lu M J, Wang B R, Chai R Q, Li L, Cai D, Yang H, Liu B K, Zhang Y P, Han W. Uncover the mystery of high-performance aqueous zinc-ion batteries constructed by oxygen-doped vanadium nitride cathode: Cationic conversion reaction works[J]. Energy Storage Mater., 2021, 35: 679-686.

[56] Peng Y Y, Yu M M, Zhao L, Ji X W, He T Q, Liu Y, Wang Q, Ran F. 3D layered nanostructure of vanadium nitrides quantum dots@graphene anode materials via *in-situ* redox reaction strategy[J]. Chem. Eng. J., 2021, 417: 129267.

[57] Niu Y, Xu W Q, Ma Y J, Gao Y, Li X L, Li L D, Zhi L J. Layer-by-layer stacked vanadium nitride nanocrystals/N-doped carbon hybrid nanosheets toward high-performance aqueous zinc-ion batteries[J]. Nanoscale, 2022, 14(20): 7607-7612.

[58] Fang G Z, Liang S Q, Chen Z X, Cui P X, Zheng X S, Pan A Q, Lu B G, Lu X H, Zhou J. Simultaneous cationic and anionic redox reactions mechanism enabling high-rate long-life aqueous zinc-ion battery[J]. Adv. Funct. Mater., 2019, 29(44): 1905267.

[59] Du W Y, Miao L, Song Z Y, Zheng X W, Lv Y K, Zhu D Z, Gan L H, Liu M X. Kinetics-driven design of 3D VN/Mxene composite structure for superior zinc storage and charge transfer[J]. J. Power Sources, 2022, 536: 231512.

[60] Park J S, Wang S E, Jung D S, Lee J K, Kang Y C. Nano-confined vanadium nitride in 3D porous reduced graphene oxide microspheres as high-capacity cathode for aqueous zinc-ion batteries[J]. Chem. Eng. J., 2022, 446: 137266.

[61] Chen H Z, Yang Z H, Wu J, Rong Y, Deng L. Industrial VN@reduced graphene oxide cathode for aqueous zinc ion batteries with high rate capability and long cycle stability[J]. J. Power Sources, 2021, 507: 230286.

[62] Li X L, Ma L T, Zhao Y W, Yang Q, Wang D H, Huang Z D, Liang G J, Mo F N, Liu Z X, Zhi C Y. Hydrated hybrid vanadium oxide nanowires as the superior cathode for aqueous Zn battery[J]. Mater. Today Energy, 2019, 14: 100361.

[63] Javed M S, Lei H, Wang Z L, Liu B T, Cai X, Mai W J. 2D V_2O_5 nanosheets as a binder-free high-energy cathode

for ultrafast aqueous and flexible Zn-ion batteries[J]. Nano Energy, 2020, 70: 104573.

[64] Yao Z G, Wu Q P, Chen K Y, Liu J J, Li C L. Shallow-layer pillaring of a conductive polymer in monolithic grains to drive superior zinc storage via a cascading effect[J]. Energy Environ. Sci., 2020, 13(9): 3149-3163.

[65] Li X L, Li M, Yang Q, Liang G J, Huang Z D, Ma L T, Wang D H, Mo F N, Dong B B, Huang Q, Zhi C Y. *In situ* electrochemical synthesis of mxenes without acid/alkali usage in/for an aqueous zinc ion battery[J]. Adv. Energy Mater., 2020, 10(36): 2001791.

[66] Venkatkarthick R, Rodthongkum N, Zhang X Y, Wang S M, Pattananuwat P, Zhao Y S, Liu R P, Qin J Q. Vanadium-based oxide on two-dimensional vanadium carbide mxene (V_2O_x@V_2CT_x) as cathode for rechargeable aqueous zinc-ion batteries[J]. ACS Appl. Energy Mater., 2020, 3(5): 4677-4689.

[67] Chen J, Xiao B Q, Hu C F, Chen H D, Huang J J, Yan D, Peng S L. Construction strategy of VO_2@V_2C 1D/2D heterostructure and improvement of zinc-ion diffusion ability in VO_2(B)[J]. ACS Appl. Mater. Inter., 2022, 14(25): 28760-28768.

[68] Sha D W, Lu C J, He W, Ding J X, Zhang H, Bao Z H, Cao X, Fan J C, Dou Y, Pan L, Sun Z M. Surface selenization strategy for V_2CT_x Mxene toward superior Zn-ion storage[J]. ACS Nano, 2022, 16(2): 2711-2720.

[69] Wang J, Wang L, Yang S B. VN Quantum dots anchored uniformly onto nitrogen-doped graphene as efficient electrocatalysts for oxygen reduction reaction[J]. Nano, 2018, 13(4): 1850041.

[70] Pu X M, Song T B, Tang L B, Tao Y Y, Cao T, Xu Q J, Liu H M, Wang Y G, Xia Y Y. Rose-like vanadium disulfide coated by hydrophilic hydroxyvanadium oxide with improved electrochemical performance as cathode material for aqueous zinc-ion batteries[J]. J. Power Sources, 2019, 437: 226917.

[71] Ding J W, Gao H G, Liu W Q, Wang S W, Wu S D, Fang S M, Cheng F Y. Operando constructing vanadium tetrasulfide-based heterostructures enabled by extrinsic adsorbed oxygen for enhanced zinc ion storage[J]. J. Mater. Chem. A, 2021, 9(18): 11433-11441.

[72] Liu J Y, Long J W, Shen Z H, Jin X, Han T L, Si T, Zhang H G. A self-healing flexible quasi-solid zinc-ion battery using all-in-one electrodes[J]. Adv. Sci., 2021, 8(8): 2004689.

[73] Xu J, Liu Y B, Chen P L, Wang A, Huang K J, Fang L X, Wu X. Interlayer-expanded VS_2 nanosheet: Fast ion transport, dynamic mechanism and application in Zn^{2+} and Mg^{2+}/Li^+ hybrid batteries systems[J]. J. Colloid. Interface Sci., 2022, 620: 119-126.

[74] Rong Y, Chen H Z, Wu J, Yang Z H, Deng L, Fu Z M. Granular vanadium nitride (VN) cathode for high-capacity and stable zinc-ion batteries[J]. Ind. Eng. Chem. Res., 2021, 60(24): 8649-8658.

[75] Su Q S, Rong Y, Chen H Z, Wu J, Yang Z H, Deng L, Fu Z M. Carbon-doped vanadium nitride used as a cathode of high-performance aqueous zinc ion batteries[J]. Ind. Eng. Chem. Res., 2021, 60(33): 12155-12165.

[76] Chen H Z, Yang Z H, Wu J. Vanadium nitride@nitrogen-doped graphene as zinc ion battery cathode with high rate capability and long cycle stability[J]. Ind. Eng. Chem. Res., 2022, 61(8): 2955-2962.

[77] Narayanasamy M, Kirubasankar B, Shi M J, Velayutham S, Wang B, Angaiah S, Yan C. Morphology restrained growth of V_2O_5 by the oxidation of V-Mxenes as a fast diffusion controlled cathode material for aqueous zinc ion batteries[J]. Chem. Commun., 2020, 56(47): 6412-6415.

[78] Rastgoo-Deylami M, Esfandiar A. High energy aqueous rechargeable nickel-zinc battery employing hierarchical NiV-LDH nanosheet-built microspheres on reduced graphene oxide[J]. ACS Appl. Energy Mater., 2021, 4(3): 2377-2387.

[79] Liu Y, Jiang Y, Hu Z, Peng J, Lai W H, Wu D L, Zuo S W, Zhang J, Chen B, Dai Z W, Yang Y G, Huang Y, Zhang W, Zhao W, Zhang W, Wang L, Chou S L. *In-situ* electrochemically activated surface vanadium valence in V_2C mxene to achieve high capacity and superior rate performance for Zn-ion batteries[J]. Adv. Funct. Mater., 2020, 31(8): 2008033.

[80] Zhu X D, Cao Z Y, Wang W J, Li H J, Dong J C, Gao S P, Xu D X, Li L, Shen J F, Ye M X. Superior-performance aqueous zinc-ion batteries based on the *in situ* growth of MnO_2 nanosheets on V_2CT_x Mxene[J]. ACS Nano, 2021, 15(2): 2971-2983.

[81] Karapidakis E, Vernardou D. Progress on V_2O_5 cathodes for multivalent aqueous batteries[J]. Mater., 2021, 14(9), 2310.

[82] Lewis C E M, Fernando J F S, Siriwardena D P, Firestein K L, Zhang C, von Treifeldt J E, Golberg D V. Vanadium-containing layered materials as high-performance cathodes for aqueous zinc-ion batteries[J]. Adv. Mater. Technol., 2021, 7(4): 2100505.

[83] Liu Y, Wu X. Review of vanadium-based electrode materials for rechargeable aqueous zinc ion batteries[J]. J. Energy Chem., 2021, 56: 223-237.

[84] Shi Y C, Chen Y, Shi L, Wang K, Wang B, Li L, Ma Y

M, Li Y H, Sun Z H, Ali W, Ding S J. An overview and future perspectives of rechargeable zinc batteries[J]. Small, 2020, 16(23): 2000730.

[85] Zhang W W, Zuo C L, Tang C, Tang W, Lan B X, Fu X D, Dong S J, Luo P. The current developments and perspectives of V_2O_5 as cathode for rechargeable aqueous zinc-ion batteries[J]. Energy Technol., 2020, 9(2): 2000789.

[86] Sui D, Wu M N, Shi K Y, Li C L, Lang J W, Yang Y L, Zhang X Y, Yan X B, Chen Y S. Recent progress of cathode materials for aqueous zinc-ion capacitors: Carbon-based materials and beyond[J]. Carbon, 2021, 185: 126-151.

[87] Jia X X, Liu C F, Neale Z G, Yang J H, Cao G Z. Active materials for aqueous zinc ion batteries: Synthesis, crystal structure, morphology, and electrochemistry[J]. Chem. Rev., 2020, 120(15): 7795-7866.

[88] Liu Z X, Sun H M, Qin L P, Cao X X, Zhou J, Pan A Q, Fang G Z, Liang S Q. Interlayer doping in layered vanadium oxides for low-cost energy storage: Sodium-ion batteries and aqueous zinc-ion batteries[J]. ChemNanoMat, 2020, 6(11): 1553-1566.

[89] Xu X M, Xiong F Y, Meng J S, Wang X P, Niu C J, An Q Y, Mai L Q. Vanadium-based nanomaterials: A promising family for emerging metal-ion batteries[J]. Adv. Funct. Mater., 2020, 30(10): 1904398.

[90] Fu Q, Wang J Q, Sarapulova A, Zhu L H, Missyul A, Welter E, Luo X L, Ding Z M, Knapp M, Ehrenberg H, Dsoke S. Electrochemical performance and reaction mechanism investigation of V_2O_5 positive electrode material for aqueous rechargeable zinc batteries[J]. J. Mater. Chem. A, 2021, 9(31): 16776-16786.

[91] Fan L, Ru Y, Xue H G, Pang H, Xu Q. Vanadium-based materials as positive electrode for aqueous zinc-ion batteries[J]. Adv. Sustain. Syst., 2020, 4(12): 2000178.

[92] Bensalah N, De Luna Y. Recent progress in layered manganese and vanadium oxide cathodes for Zn-ion batteries [J]. Energy Technol., 2021, 9(5): 2100011.

[93] Zhao J, Ren H, Liang Q H, Yuan D, Xi S B, Wu C, Manalastas W, Ma J M, Fang W, Zheng Y, Du C F, Srinivasan M, Yan Q Y. High-performance flexible quasi-solid-state zinc-ion batteries with layer-expanded vanadium oxide cathode and zinc/stainless steel mesh composite anode[J]. Nano Energy, 2019, 62: 94-102.

[94] Wang X W, Wang L Q, Zhang B, Feng J M, Zhang J F, Ou X, Hou F, Liang J. A flexible carbon nanotube@V_2O_5 film as a high-capacity and durable cathode for zinc ion batteries[J]. J. Energy Chem., 2021, 59: 126-133.

[95] Alfaruqi M H, Mathew V, Song J J, Kim S, Islam S, Pham D T, Jo J, Kim S, Baboo J P, Xiu Z, Lee K S, Sun Y K, Kim J. Electrochemical zinc intercalation in lithium vanadium oxide: A high-capacity zinc-ion battery cathode[J]. Chem. Mater., 2017, 29(4): 1684-1694.

[96] He P, Yan M Y, Liao X B, Luo Y Z, Mai L Q, Nan C W. Reversible V^{3+}/V^{5+} double redox in lithium vanadium oxide cathode for zinc storage[J]. Energy Storage Mater., 2020, 29: 113-120.

关于水系锌离子电池中无氧钒基正极材料的综述

贠潇如, 陈宇方*, 肖培涛*, 郑春满*

(国防科技大学空天科学学院, 湖南 长沙 410073)

摘要: 水系锌离子电池具有功率密度高、环境友好、安全性高、低成本和锌资源丰富等优点，被认为具有潜力成为下一代电化学储能系统。然而，正极材料较差的电化学性能制约了水系锌离子电池的未来发展。尽管氧化锰、氧化钒、普鲁士蓝类似物、有机材料等多种材料已被广泛研究，设计具有高性能的理想正极材料仍面临着巨大挑战。无氧钒基化合物由于具有高的电导率、大的层间距、低的离子扩散势垒和高的理论比容量，受到越来越多的关注。本文总结了无氧钒基化合物的研究进展，包括电极材料的设计、改善其电化学性能的有效途径以及复杂的储能机制，提出了无氧钒基化合物目前面临的挑战和未来的发展前景，为进一步制备新型高性能钒基正极材料提供指导。

关键词: 锌离子电池; 无氧钒基化合物; 储能机制; 电化学性能